JGP Journal of General Physiology

REVIEW

ATP synthase: Evolution, energetics, and membrane interactions

Jasmine A. Nirody[1,2], Itay Budin[3], and Padmini Rangamani[4]

The synthesis of ATP, life's "universal energy currency," is the most prevalent chemical reaction in biological systems and is responsible for fueling nearly all cellular processes, from nerve impulse propagation to DNA synthesis. ATP synthases, the family of enzymes that carry out this endless task, are nearly as ubiquitous as the energy-laden molecule they are responsible for making. The F-type ATP synthase (F-ATPase) is found in every domain of life and has facilitated the survival of organisms in a wide range of habitats, ranging from the deep-sea thermal vents to the human intestine. Accordingly, there has been a large amount of work dedicated toward understanding the structural and functional details of ATP synthases in a wide range of species. Less attention, however, has been paid toward integrating these advances in ATP synthase molecular biology within the context of its evolutionary history. In this review, we present an overview of several structural and functional features of the F-type ATPases that vary across taxa and are purported to be adaptive or otherwise evolutionarily significant: ion channel selectivity, rotor ring size and stoichiometry, ATPase dimeric structure and localization in the mitochondrial inner membrane, and interactions with membrane lipids. We emphasize the importance of studying these features within the context of the enzyme's particular lipid environment. Just as the interactions between an organism and its physical environment shape its evolutionary trajectory, ATPases are impacted by the membranes within which they reside. We argue that a comprehensive understanding of the structure, function, and evolution of membrane proteins—including ATP synthase—requires such an integrative approach.

Introduction

The use of ATP as a source of chemical energy to drive metabolic activity is ubiquitous and shared among all known cellular life-forms. The energy stored in ATP's phosphoanhydride bond is used to power a wide range of processes including muscle contraction, cell motility, nerve impulse propagation, and DNA synthesis, among many others. This impressive task list has earned the molecule the title of the "universal energy currency." As might be expected, the turnover of ATP is also remarkable: the human body uses about its weight in ATP daily (Dimroth et al., 2006), and cells must continually regenerate ATP from the products of its hydrolysis (ADP and phosphate) to keep up with this demand. ATP synthases, the enzymes that perform this tireless job, are nearly as universal as the currency they are responsible for minting.

The ATP synthase family of enzymes comprises three members: A-, V-, and F-type ATPases/ATP synthases (Kagawa and Racker, 1966; Penefsky et al., 1960). In vitro, all three are reversible: they can both use the energy of ATP hydrolysis to move cations across ion-impermeable membranes and use the energy stored in the transmembrane ion gradient to synthesize ATP. In vivo, the V type acts as an ATPase (Forgac, 2007). The A and F types can work in either direction in prokaryotes (Müller and Grüber, 2003). In eukaryotic mitochondria and chloroplasts, F-type ATPases act primarily as ATP synthases, though a notable exception is found in mammalian mitochondria, where F-type ATPases can pump ions to reenergize the membrane (Kühlbrandt, 2019).

A-type ATPases exist in archaea (Müller and Grüber, 2003), although they are also used by a small number of bacterial species, which appear to have obtained them via horizontal gene transfer (Lapierre et al., 2006). V-type ATPases belong to the eukaryotes and sit primarily in the membranes of vacuoles (Forgac, 2007). The final class, the F-type ATPases, is the only one with members found in every branch of the tree of life: present in both bacterial and mitochondrial membranes (von Ballmoos et al., 2009), they were originally characterized as coupling factors (CF-ATPases). Later, when they were discovered in chloroplasts, the "C" was dropped to avoid confusion (Kühlbrandt, 2019). The reach of F-type ATPases then extended

[1]Center for Studies in Physics and Biology, The Rockefeller University, New York, NY; [2]All Souls College, University of Oxford, Oxford, UK; [3]Department of Chemistry and Biochemistry, University of California San Diego, La Jolla, CA; [4]Department of Mechanical and Aerospace Engineering, University of California San Diego, La Jolla, CA.

Correspondence to Jasmine A. Nirody: jnirody@rockefeller.edu; Padmini Rangamani: prangamani@ucsd.edu.

to archaea when a subclass (the novel, or N type) was identified in some archaeal species—once again, thought to be a consequence of a lateral gene transfer event (Dibrova et al., 2010).

Due to their prevalence in organisms ranging from archaea to animals, we focus on diversification in F-type ATPases/ATP synthases. For ease of exposition, we will refer to this family of enzymes as ATPases in the remainder of this text. We begin with a brief overview of shared structural, functional, and phylogenetic features between the classes of ATPases. For more detailed reviews on the other members of the ATPase family, we refer interested readers to the following excellent reviews: Forgac, 2007 for V-type ATPases and Grüber et al., 2014 for A-type ATPases.

Structurally, all rotary ATPases share basic similarities: each is composed of a soluble domain (termed A1, V1, or F1 for the A, V, and F type, respectively) coupled to a membrane-embedded domain (Ao, Vo, or Fo) by a connecting stalk (Kühlbrandt, 2019). The former contains the ATP hydrolyzing/synthesizing domain, while the latter facilitates ion translocation across the membrane. Each domain on its own is an independent stepping motor; this modularity has, for instance, been demonstrated by experiments showing that detached F1 and A1 retain rotary movement driven by ATP (Imamura et al., 2003; Noji et al., 1997). The membrane domain is often described in terms analogous to macroscopic motors: the rotary portion of the motor is designated the "rotor," while the static portion is fixed to the soluble domain by the motor's "stator." In the "ion pump" or ATP hydrolysis mode, the soluble domain sequentially drives rotation of an "axle" that transmits energy to the membrane-embedded component; when in the "power" or ATP synthesis mode, ion movement through the membrane domain drives axle rotation (Muench et al., 2011).

Based on sequence and subunit composition, A-type ATPases are more closely related to V-type ATPases than to F-type ATPases. Functionally, however, the A and F types show more similarities—for instance, the ability to synthesize ATP in vivo (Iwabe et al., 1989; Ihara et al., 1992; Müller et al., 1999; Schäfer et al., 1999). These similarities in sequence, structure, and function point to the existence of a shared common ancestor, which underwent a series of changes to arrive at the three modern ATPase classes (Imamura et al., 2003; Zimniak et al., 1988). Due to the conservation of their basic structure and function across biological kingdoms, the ATP synthases are an intriguing framework within which to study several major events in the evolution of life, from its origin and the rooting of the tree of life (Mulkidjanian et al., 2009) to the prokaryote–eukaryote transition (Hilario and Gogarten, 1998), among others. There have been several excellent pieces of work on the diversity of ATPases, which use sequence data, high-resolution structures, and functional assays (von Ballmoos et al., 2009; Muench et al., 2011; Müller and Grüber, 2003).

However, the dynamics of diversification in the ATPase lineage must take into account the "ecology" of these enzymes: just as the interactions between an organism and its physical environment shapes its evolutionary trajectory, ATPases do not perform their duties in a vacuum. Indeed, there is evidence of coevolution between biological membranes and membrane proteins, suggesting that a deeper understanding of the evolutionary history of the ATPases may provide key insights into the prototypic organism from which sprouted the tree of life (see, e.g., Mulkidjanian et al., 2009). Studies have shown how ATP synthase dimers can shape mitochondrial cristae (Seelert and Dencher, 2011); dimers have been observed in a small fraction of chloroplast ATP synthases as well, though likely through an independent mechanism (Daum et al., 2010; Rexroth et al., 2004).

There are myriad adaptations that have allowed ATPases to drive the survival of organisms in such a wide range of environments—many that have yet to be fully characterized, and too many to squeeze into even the most exhaustive review. Here, we begin with a comparative overview of the structure and function of F-type ATPases in mitochondria, chloroplasts, and prokaryotes (here, we group together the bacteria and archaeal enzymes due to their purported common origin). We then discuss several adaptations that have been observed across species, either via a shared ancestor or through convergent evolution.

F-ATPase structure and function across biological domains

Like their siblings, F-ATPases are "dual motors," composed of two modular units, the cytoplasmic F1 and the membrane-embedded Fo. Prokaryotic and chloroplast ATPases are relatively simple in structure, while mitochondrial enzymes are more complex and variable between species and cell types; a comparison of these structures is provided in Fig. 1.

The catalytic F1 "head," the site of ATP synthesis, is a mushroom-shaped extension that pokes ∼11 nm into the cytoplasm. The F1 subunit comprises three α- and three β-subunits arranged around a central γ-subunit. As F1's membrane-bound counterpart, the Fo sector is responsible for torque generation during synthesis (power mode) and for ion translocation in ion pump mode, the reverse direction (Walker, 1998). The membrane-bound motor contains the a-subunit and a "rotor ring" of 8–17 c-subunits, depending on the species (Meier et al., 2005a, 2005b). The geometry of the side chains of the c-ring determine the ion selectivity in bacterial motors (Dimroth, 1997; Krah et al., 2010)—that is, whether the motor runs on the proton motive force (pmf) or the sodium motive force (smf).

The F1 and Fo sectors are connected by two stalks: one central, composed of subunits γ and ε, with the additional δ in mitochondria; and one peripheral, composed of the b-subunits, and with the additional d-subunit and F6 in mitochondria (Wilkens and Capaldi, 1998). The central stalk is responsible for transferring torque generated by Fo to the catalytic F1 head, shifting it between the three conformations shown in Fig. 2. The ε-subunit has also been shown to have some regulatory functions in bacteria and chloroplasts (Feniouk et al., 2006; Gibbons et al., 2000; Laget and Smith, 1979; Richter et al., 1984; Smith et al., 1975; Stock et al., 2000); additionally, in chloroplasts, the γ-subunit acts as a regulator to switch off nighttime ATPase activity (Kohzuma et al., 2013). Mitochondrial ATPases are regulated by a separate small inhibitory protein IF1 (Bason et al., 2014; Gledhill et al., 2007; Pullman and Monroy, 1963). The peripheral stalk is connected to F1 by the δ-subunit in chloroplasts (unrelated to the δ-subunit in the mitochondrial central stalk,

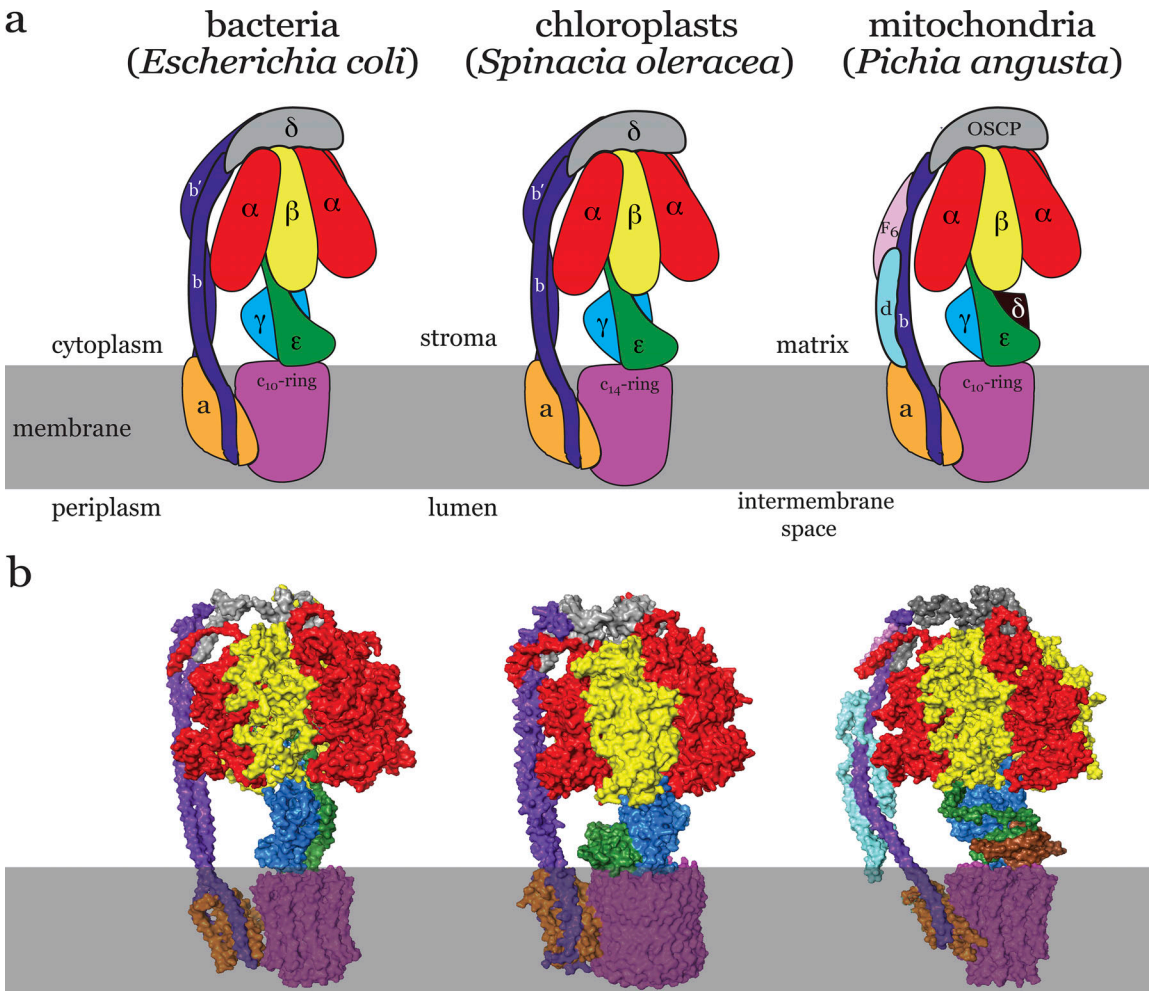

Figure 1. **Comparative schematic and atomic models of F1Fo motors from bacteria, chloroplasts, and mitochondria.** Map resolutions are as follows: 6.9 Å for *E. coli* ATP synthase (Sobti et al., 2016); 2.9 Å/3.4 Å for *Spinacia oleracea* (spinach) chloroplast F1/Fo, respectively (Hahn et al., 2018); and 7.0 Å for *Pichia angusta* mitochondrial ATP synthase (Vinothkumar et al., 2016). Subunits are color coded to show homologous domains across species: α (red); β (yellow), δ (gray in bacteria and chloroplasts, brown in mitochondria); OSCP (gray in mitochondria); b/b′ (dark purple); c-ring (light purple); F6 (pink); γ (blue); ε (green); and d (light blue).

except through a confusing naming convention!) and by the oligomycin sensitivity conferral protein (OSCP) in mitochondria. Sequence studies indicate that the δ-subunit and OSCP are nearly the same protein, indicating that the peripheral stalk has remained unchanged for over 1.5 billion years (Hohmann-Marriott and Blankenship, 2011; Rand et al., 2004).

The catalytic sites in the F1 sector, where the nucleotides bind, are contained mostly in the β-subunits, with the α-subunits contributing an essential arginine residue. These sites go from being empty (βE) to being occupied by Mg-ADP and phosphate (βDP). Driven by the current flow through Fo, F1 can catalyze these ligands to form Mg-ATP at the third catalytic site (βTP; Gibbons et al., 2000; Stock et al., 2000). When operating in the other direction (ion pump mode), the catalysis of Mg-ATP drives rotation of the c-unit via the central stalk, facilitating the transmembrane flow of ions (Junge at al., 1997; Cherepanov et al., 1999; Feniouk et al., 2004; Mulkidjanian et al., 2007).

The three rotational states in the F1 sector were resolved through high-resolution cryo-EM studies in bacteria (in *Escherichia coli*, Sobti et al., 2016; and *Bacillus* PS3, Guo et al., 2019) and chloroplasts (in spinach, Hahn et al., 2018). Using fluorescently labeled bacterial F1, the γ-subunit was shown to rotate at >130 Hz, indicating that bacterial F-ATPases can synthesize (or hydrolyze) ~400 molecules of ATP every second (Fischer et al., 1994; Yasuda et al., 2001)! The OSCP region has been shown to be responsible for the flexible coupling between the two sectors, consolidating F1's three discrete catalytic steps with Fo's more continuous rotation (Murphy et al., 2019). A schematic of this cycle, termed the binding change mechanism (Boyer, 1997; Boyer at al., 1977), is shown in Fig. 3. Several theoretical models have been posed, at varying levels of abstraction, to describe this mechanism (Elston et al., 1998; Mukherjee and Warshel, 2012; Oster et al., 2000; Oster and Wang, 2000; Sun et al., 2004; Wang and Oster, 1998; Xing et al., 2005).

Fueling up: Selective ion binding and transport

The vast majority of extant metabolic strategies are believed to have been in stasis after their emergence in the first billion years

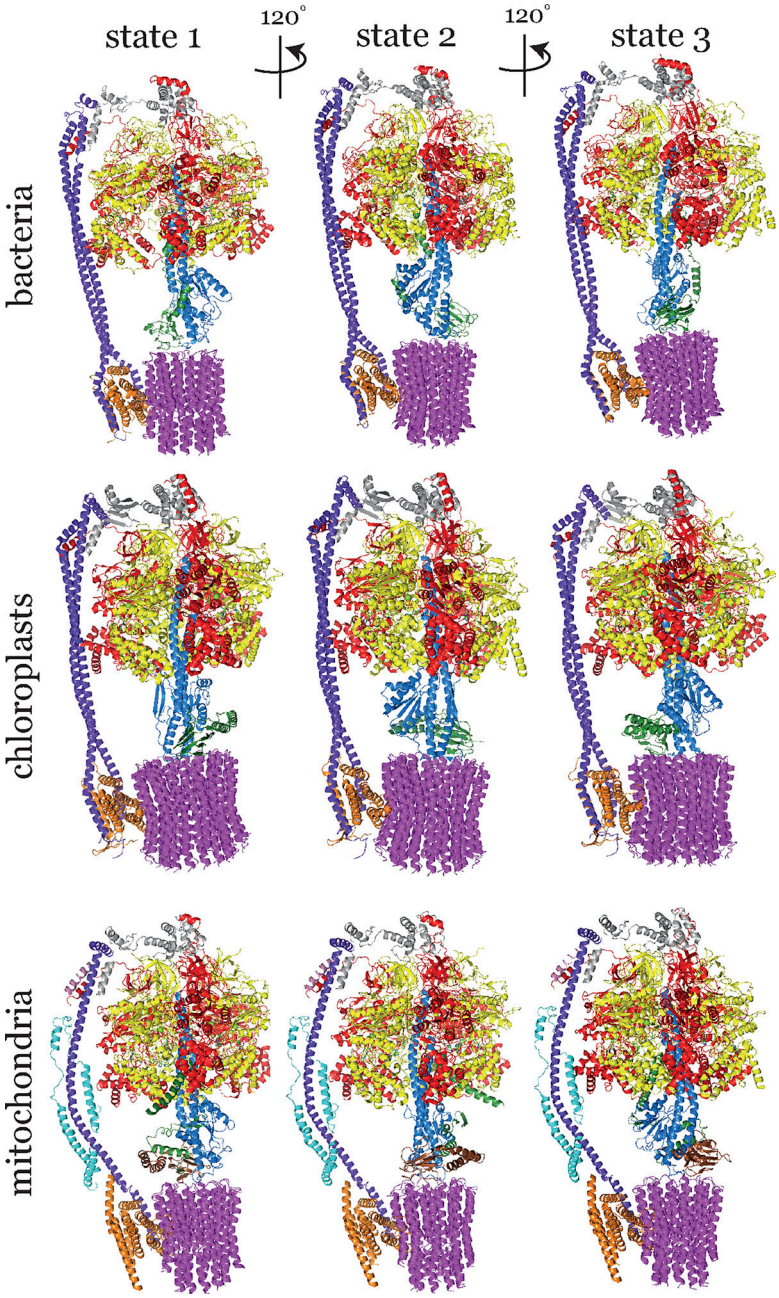

Figure 2. **Three primary rotary states of intact F1Fo ATPases in bacteria (*E. coli*), chloroplasts (*S. oleracea*), and mitochondria (*P. angusta*), separated by an ∼120° rotation.** States are listed from most to least populated; the most populated states for each organism (conformation 1) are as shown in Fig. 1.

after the origin of life on Earth (Banfield and Marshall, 2000; Battistuzzi et al., 2004; Knoll and Bauld, 1989). Despite this concentrated time scale, organisms have developed many ways to make and use energy, including aerobic and anaerobic respiration, methanogenesis, sulfur and iron reduction or oxidation, and several others (Boucher et al., 2003; Castresana, 2001; Koumandou and Kossida, 2014; Reysenbach and Shock, 2002).

The diversity of these metabolic modes is perhaps most obvious in the prokaryotes. Interestingly, these pathways exhibit a "patchy distribution" across the prokaryotic phylogeny, indicating >25 independent origins or over a dozen horizontal gene transfer events. However, there is no such evidence of such "patchiness" in the universal enzyme central to all these pathways: F-ATPase. A phylogenetic analysis of all the subunits of F-ATPase showed that enzyme sequence and structure did not cluster with bioenergetic mode. This analysis confirms the widespread utilization, and thus ancient origin, of ATP synthase. Importantly, it also points to its robustness: F-ATPase, showing few specific modifications, is able to function as part of a wide variety of electron transport chains (ETCs) and within a wide variety of cell types (Koumandou and Kossida, 2014).

One of the most basic questions one can ask about an ion-driven enzyme is about its choice of fuel. For ATP synthases, however, this question has also proven to be one of the most puzzling. Environmental factors, such as temperature or pH, have not been found to consistently determine several features of ATP synthases, including ion selectivity. Under most physiological conditions, the Na^+ gradient far surpasses that of H^+—often by a millionfold (e.g., in the mitochondria) or more (e.g., in alkaline environments). But despite this environmental bias,

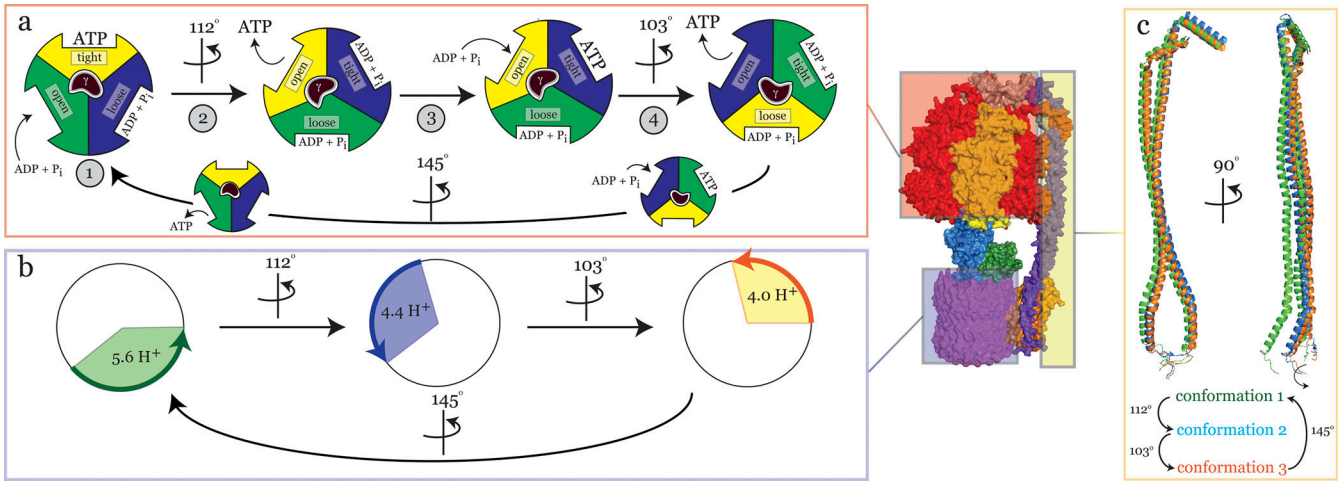

Figure 3. **Illustration of one full revolution of chloroplast F1, Fo, and the peripheral stalk connection between the two motors.** As shown in Fig. 2, image processing revealed three primary rotary states in intact chloroplast F-ATPase, separated by 112°, 103°, and 145° (Hahn et al., 2018). **(a)** A full revolution of F1 results in the generation of three ATP molecules, one at each of the three catalytic β-subunits via Paul Boyer's proposed "binding change mechanism" (Boyer, 1993; Boyer, 1997; Boyer at al., 1977). The three β-subunits cycle between "open," "tight," and "loose" states. Tracking a single β-subunit through a full revolution: (1) ADP + Pi arrive and bind at the open site; (2) upon arrival of ADP and phosphate, the open subunit rotates into the loose conformation, followed by (3) a second rotary power stroke into the tight conformation, in which the catalysis into ATP takes place. (4) The final substep reverts the subunit back to its open conformation, releasing the newly synthesized ATP. **(b)** Rotation angles of the Fo c-ring rotor relative to subunit a. Primary states of the intact motor do not each correspond to an integral number of c-subunits (and consequently, neither to an integral number of ion translocations). **(c)** Two orthogonal views of superposed peripheral stalks, illustrating the flexible coupling between Fo and F1; this flexibility allows for the observed "symmetry mismatch" between the paired motors (see Fig. 4).

nearly all F-ATPases (and their V-type siblings) use proton flow as their power source. Structurally, membrane proteins within the same family driven by pmf or smf are largely conserved (Meier et al., 2005a; Yamashita et al., 2005; Pogoryelov et al., 2009; Ressl et al., 2009; Ethayathulla et al., 2014), indicating that "switching" between these two energy sources occurs via localized changes in amino acid composition rather than any dramatic structural modifications (Leone et al., 2015). It is somewhat surprising, then, that the strong H^+ selectivity required to counteract the environmental sodium excess is achievable through such minor modifications.

Ion specificity in ATP synthases is the domain of the membrane-embedded Fo sector. The a-subunit provides an aqueous pathway for ion transport onto binding sites along the ring of c-subunits (Angevine et al., 2003; Steed and Fillingame, 2008; Steed and Fillingame, 2009). To date, bioinformatic and experimental studies have indicated that the a-subunit does not provide any specificity to the enzyme, relegating the responsibility of ion choice to the c-ring (Dimroth et al., 2006; Schlegel et al., 2012; Stock et al., 2000; Weber and Senior, 2003). Extensive work on c-rings from both Na^+- and H^+-driven enzymes suggests that all ATPases select H^+ over Na^+, and that H^+ selectivity is an ancestral feature of the F-ATPases (Krah et al., 2010; Leone et al., 2015; Meier et al., 2009; Pogoryelov et al., 2009).

This baseline selectivity, however, is neither strong enough to overcome the Na^+ excess in extant natural environments nor weak enough to reliably and exclusively couple the enzyme to sodium flow. Therefore, any form of ion selectivity—that is, any nonpromiscuous coupling to either pmf or smf—requires a deviation from the baseline state: to enhance Na^+ binding, the binding sites tend toward a higher number of polar amino acids; to favor H^+, the sites become more hydrophobic (Krah et al., 2010; Leone et al., 2015; Schulz et al., 2013). Shifts in both directions have been well characterized across a wide range of bacteria and archaea. For instance, in the alkalophilic bacterium *Bacillus pseudofirmus*, the only hydrophilic residue around the binding sites is the conserved Glu, which is common to all F-ATPases (Pogoryelov et al., 2009; Symersky et al., 2012; Vollmar et al., 2009; Zhou et al., 2015), leading to a strong H^+ selectivity (Preiss et al., 2010; Schlegel et al., 2012). Swinging to the other extreme, the well-characterized physiological Na^+ coupling in the bacterial species *Ilyobacter tartaricus* and *Enterococcus hirae* arises from three cation-coordinating polar side chains (Meier et al., 2009; Schlegel et al., 2012). A broader overview of the spectrum of ion selectivity across the prokaryotic phylogeny is provided in Fig. 4.

Ion flow across biological membranes maintains a wide range of processes in all living cells, from archaea to humans. Of these, one of the first, and most fundamental, is ATP synthesis. Understanding the origin and evolution of bioenergetics therefore relies crucially on the mechanisms adapted by ATP synthases to couple their function to distinct energy sources. Despite the bias toward H^+ selectivity in most extant organisms (including all eukaryotes), Na^+-dependent ATPases are scattered among many branches of the phylogenetic tree. Given the specific identity of the Na^+ binding sites across lineages (Mulkidjanian et al., 2009), this provides compelling evidence for the evolutionary primacy of sodium bioenergetics.

A potential implication of an ancestral Na^+-dependent ATPase is that the predecessor of modern proton- and sodium-impermeable membranes could have been sodium impermeable but proton permeable. One model for early cell evolution is

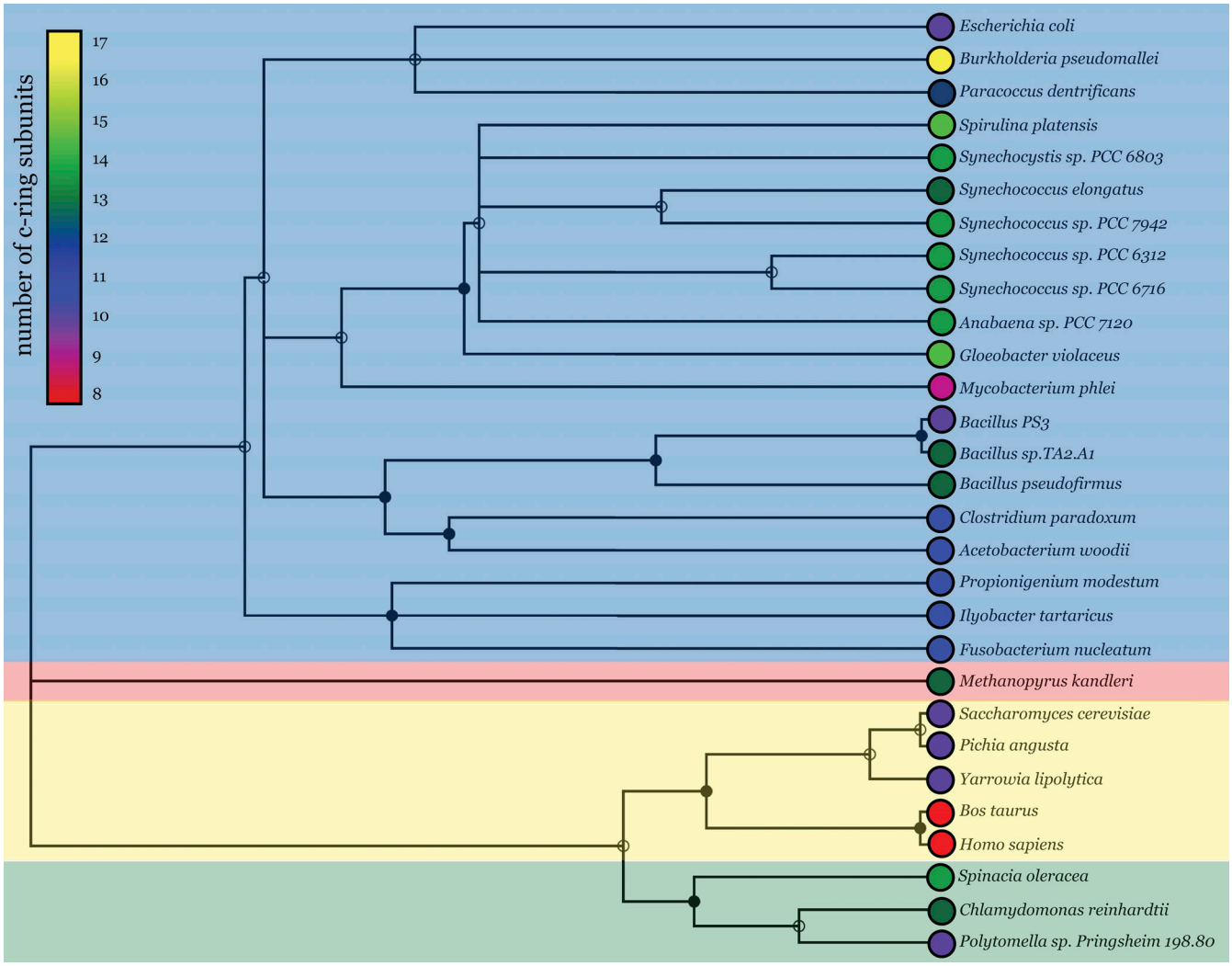

Figure 4. **Phylogenetic distribution of c-ring stoichiometries.** Rooted phylogeny of organisms with experimentally determined c-ring structures obtained through the TimeTree knowledge base using the method outlined in Hedges et al., 2015. Leaves are marked with colored circles according to the number of subunits found in the ATP synthase c-ring. Shading corresponds to whether stoichiometries were determined for bacteria (blue), archaea (red), eukaryotic mitochondria (yellow), or chloroplasts (green). Stoichiometries and corresponding references are also provided in Table 1.

that membranes made from single-chain amphiphiles, such as fatty acids and their derivatives, gradually transitioned to those made from phospholipids (Budin and Szostak, 2011). Fatty acids can be synthesized abiotically and self-assemble into membrane vesicles (Hargreaves and Deamer, 1978) that are capable of spontaneous growth and division (Zhu and Szostak, 2009). Membrane-bound fatty acids switch between deprotonated and protonated forms, with the latter being neutral and capable of rapid (approximately milliseconds) flip-flop (Kamp et al., 1995). Through cycles of flip-flop and proton release, fatty acids thus act as protonophores. In contrast, ion permeation in pure phospholipid membranes is mediated by direct ion partitioning or formation of transient pores in the bilayer (Paula et al., 1996). For this reason, free fatty acids act as natural uncouplers in mitochondria (Di Paola and Lorusso, 2006). Fatty acids can also transport sodium and other larger cations as salts, but much more slowly than for protons (Chen and Szostak, 2004). Thus, proton-based bioenergetics could have been a challenge for primitive cell membranes with substantial amounts of free fatty acids or high intrinsic leakiness, thus favoring the early utilization of sodium as a less permeable cation. The coupling of transmembrane proton flow to bioenergetic cellular processes would have then arisen later, and on several independent occasions, along life's evolutionary path (Mulkidjanian et al., 2009).

Despite much progress in our understanding of membrane mechanics and bioenergetics in recent years, the origin and evolution of biomembranes and the proteins that live within them remain an open question, into which the reconstruction of ATP synthase evolution can provide insight (Mulkidjanian et al., 2009).

If the ring fits: Variation in rotor size and stoichiometry

During ATP synthesis, the Fo motor converts the energy stored in the transmembrane ion gradient (either the pmf or smf, as discussed in the previous section) into torque against the catalytic F1 head (Junge et al., 2009; Martin et al., 2018). In reverse,

the F1 head uses the chemical energy released from ATP hydrolysis into torque against Fo, converting its partner into an ion pump (Noji et al., 1997). Whichever way the wheels are turning, a revolution of F1 is tightly coupled mechanically to a revolution of Fo via the central stalk. Across species and cell types, the F1 head invariably contains three catalytic b-subunits and accordingly completes its revolution in three 120° steps, or "power strokes" (Martin et al., 2018). The intermediate rotary states, then, are determined by the stoichiometry of Fo's rotor ring; that is, the number of c-subunits (n) that make up the ring.

This nearly always leads to a symmetry mismatch, as n is rarely a multiple of three; one of the rare exceptions to this seems to be the c15 ring of the alkalophilic bacterium *Streptomyces platensis* (Pogoryelov et al., 2005). This, as might be expected, leads to rotary states that are not separated by exactly 120° (Hahn et al., 2018). Instead, the three steps are postulated to represent local energy minima in the catalytic cycle that take into account the whole F1–Fo complex; as such, they also often do not correspond to integral numbers of c-subunits. For example, experiments on the autoinhibited chloroplast ATP synthase showed three primary rotary substates separated by 103°, 112°, and 145°, corresponding to 4, 4.4, and 5.6 c-subunits, respectively (Hahn et al., 2018).

Each c-subunit contains one binding site for a membrane-crossing ion and translocates one ion per revolution—or per ATP synthesized or hydrolyzed. Due to the tight coupling between the two motors, the stoichiometry of the rotor ring, the number of c-subunits, theoretically determines the ratio of ions per ATP (n/3). The free energy of ATP hydrolysis ΔG is approximately −50 kJ/mol; taking into account the energetic environment in the spinach chloroplast, transitioning between the three primary substates listed above corresponds to free energy changes of −43.7, −48.1, and −61.2 kJ/mol (Hahn et al., 2018; Kühlbrandt, 2019). The primary substates in *E. coli* ATP synthase were shown to hold to a similar principle (Hahn et al., 2018; Yanagisawa and Frasch, 2017). In mitochondria, the ion-to-ATP coupling ratio is related to the P/O ratio, the number of ATP synthesized for each pair of electrons (Ferguson, 2010).

Rotor ring stoichiometry ranges from 8 c-ring subunits in mammalian mitochondria (Zhou et al., 2015; Watt et al., 2010) to 17 in the human pathogen *Burkholderia pseudomallei* (Schulz et al., 2017). In bacteria, this stoichiometry was shown to be independent of growth conditions (Pogoryelov et al., 2012). Based on an analysis of the primary structure of ATP synthase c-subunits, ring size was shown to depend on the sequence of amino acids in the contact region between adjacent subunits; this interaction motif is a highly conserved set of glycine (or sometimes alanine) repeats, GxGxGxGxG, in the N-terminal α-helix (MacKenzie et al., 1997; Preiss et al., 2013; Preiss et al., 2014). This sequence is genetically programmed, which explains why c-ring stoichiometry is fixed for members of a given species, even as it varies across different species (see Table 1 and Fig. 4).

The number of c-subunits in the rotor ring seems to be an adaptation to the physiological environment the ATPase resides in. For instance, the large c-ring in *B. pseudomallei* has a high ion-to-ATP ratio, making the enzyme an efficient ion pump and allowing the pathogen to deal with the hostile acidic host phagosome (Schulz et al., 2017). The overwhelming majority of studies have demonstrated that c-ring stoichiometries within a given species do not vary with external conditions like medium pH, host membrane composition, or carbon source (Meier and Dimroth, 2002; Meyer zu Tittingdorf et al., 2004; Meier et al., 2005b, 2007; Fritz et al., 2008; Davis and Kramer, 2020; but see also, e.g., Schemidt et al., 1998). However, genetically engineered rotors of modified size have been shown to function in both "directions" within their host cell—that is, edited F1–Fo complexes can both synthesize and hydrolyze ATP. Further, spectroscopic evidence in *I. tartaricus* (wild type n = 11) implies that the central stalk can interact with rotor rings comprised of a range of c-subunits ($11 < n < 15$) with affinity comparable to that of the wild type (Pogoryelov et al., 2012). Biochemical and structural evidence also suggest that single mutants in the c-subunit of F-ATPases can alter rotor ring stoichiometry; studies suggest that evolutionary adaptation in rotor ring size is largely independent of the mechanical coupling of Fo to the F1 head (Pogoryelov et al., 2012).

Distinct origins for F1 and Fo have long been suggested—the F1 subunit is purported to have descended from an ATP-dependent helicase, and the Fo from a passive ion channel (Falk and Walker, 1988; Gay and Walker, 1981; Gomis-Rüth et al., 2001; Havlíčková et al., 2010; Tzagoloff, 1969). Recent phylogenetic analyses have further indicated that the c-subunit may comprise an evolutionary module of its own, separate from the rest of Fo (Niu et al., 2017). This is supported by previous functional results suggesting that the c-subunit formed a "leaky" nonselective ion channel in the mitochondrial inner membrane (Alavian et al., 2014). A unique evolutionary trajectory for the c-ring is also consistent with the above discussion on the diversity in rotor ring stoichiometry. The evolutionary story of the F-ATPases is complex, and several studies have assigned a central role to the c-subunit (Havlíčková et al., 2010; Mulkidjanian et al., 2007; Niu et al., 2017; Rak et al., 2011). Understanding the history of the interactions of the c-ring with the b- and stalk subunits may provide significant insight into the integration of F1 and Fo within the ATP synthase complex (Collinson et al., 1996; Niu et al., 2017). Certainly, much further work is warranted toward understanding both the origins and currently observed diversity of the F-ATPase rotor ring.

Interestingly, changes in rotor ring size are also hypothesized to have occurred as an adaptation to selective pressure on motor torque in the bacterial flagellar motor, the only other known ion-driven rotary nanomotor. Structural modifications of the bacterial flagellar motor rotor, however, involve far more complex genetic maneuvers than in F-ATPases (Beeby et al., 2016; Chaban et al., 2018). As such, bacteria instead modify their stator stoichiometry in response to more immediate challenges (Lele et al., 2013; Nirody et al., 2019; Nord et al., 2017; Wadhwa et al., 2019). However, the relative ease of F-ATPase rotor ring modification suggests that a series of gradual changes in c-ring stoichiometry may be a feasible "strategy" to adjust ion-to-ATP ratios in novel environments within a relatively short evolutionary time scale (e.g., in host–pathogen relationships).

Table 1. **Experimentally determined rotor ring stoichiometries and ion selectivities in ATP synthases across the tree of life**

Species	Rotor size	Ion	Reference
Acetobacterium woodii	11	Na^+	Bogdanović et al., 2019
Anabaena sp. PCC 7120	14	H^+	Pogoryelov et al., 2007
Bacillus PS3	10	H^+	Mitome et al., 2004
Bacillus pseudofirmus	13	H^+	Preiss et al., 2013
Bacillus sp. TA2.A1	13	H^+	Cook et al., 2003
Bos taurus[a]	8	H^+	Giraud et al., 2012
Burkholderia pseudomallei	17	H^+	Schulz et al., 2017
Chlamydomonas reinhardtii[b]	13	H^+	Meyer zu Tittingdorf et al., 2004
Clostridium paradoxum	11	H^+	Meier et al., 2006
Escherichia coli	10	H^+	Jiang et al., 2001
Fusobacterium nucleatum	11	Na^+	Schulz et al., 2013
Gloeobacter violaceus	15	H^+	Pogoryelov et al., 2007
Homo sapiens[a]	10	H^+	Song et al., 2018
Ilyobacter tartaricus	11	Na^+	Meier et al., 2005a
Methanopyrus kandleri	13	H^+	Pogoryelov et al., 2007
Mycobacterium phlei	9	H^+	Preiss et al., 2015
Pichia angusta[a]	10	H^+	Vinothkumar et al., 2016
Paracoccus denitrificans	12	H^+	Morales-Rios et al., 2015
Polytomella sp. Pringsheim 198.80[a]	10	H^+	Leone and Faraldo-Gómez, 2016
Propionigenium modestum	11	Na^+	Meier et al., 2005b
Saccharomyces cerevisiae[a]	10	H^+	Symersky et al., 2012
Spinacia oleracea[b]	14	H^+	Hahn et al., 2018
Spirulina platensis	15	H^+	Pogoryelov et al., 2005
Synechococcus sp. PCC 6301	14	H^+	Pogoryelov et al., 2007
Synechococcus sp. PCC 6716	14	H^+	Pogoryelov et al., 2007
Synechococcus sp. PCC 7942	14	H^+	Pogoryelov et al., 2007
Synechococcus sp. SAG 89.79	13	H^+	Pogoryelov et al., 2007
Synechocystis sp. PCC 6803	14	H^+	Pogoryelov et al., 2007
Yarrowia lipolytica[a]	10	H^+	Hahn et al., 2016

Phylogenetic relationships between organisms listed are provided in Fig. 4.
[a]Mitochondria.
[b]Chloroplasts.

It takes two: Dimerization in mitochondrial ATPases

Unlike those found in prokaryotes and chloroplasts (but see, e.g., Daum et al., 2010; Rexroth et al., 2004), mitochondrial F-ATPases (mtF1Fo) all form dimers in the membrane. However, in accordance with the large variation found within the eukaryotic lineages, mitochondrial ATPases vary quite widely with respect to their subunit composition. Consequently, different dimerization strategies are used across eukaryotic taxa, with four classes of dimers having been characterized thus far: type I, found in animals and fungi (Davies et al., 2011; Davies et al., 2012; Dudkina et al., 2006; Strauss et al., 2008); type II, found in most unicellular green algae except the *Euglena*, which contain type IV dimers (Blum et al., 2019; Cano-Estrada et al., 2010; Dudkina et al., 2010; van Lis et al., 2005; van Lis et al., 2007; Vázquez-Acevedo et al., 2006); type III, found in the ciliates (Allen, 1995; Mühleip et al., 2016); and type IV, found in trypanosomes and *Euglena* (Mühleip et al., 2017). We note that, as new research is constantly plumbing new depths with respect to diversity within the unicellular eukaryotes, the discovery and classification of many more types of F-ATPase dimers is likely. There exists no apparent homology between the four classes, and the major distinction between them is the subunit composition of the dimerization interface. Variations in this interface can cause large changes in the angle observed between central stalks of the two monomeric partners, ranging from close to 0° (type III dimers; Mühleip et al., 2016) to ∼90° (type I dimers; Davies et al., 2011).

The dimerization of ATP synthase is also tied to the formation of the characteristic folds, or cristae, of the inner mitochondrial

membrane (IMM). The larger-scale organization of mtF1Fo dimers within the IMM is determined by the nature of the dimerization interface. Cryo-electron tomograms in fungi and metazoans have revealed that type I dimers are organized into long (~1 mm) rows that align themselves with the sharply curved cristae edges (Davies et al., 2012; Strauss et al., 2008). Mutation studies in yeast have concretely connected the proper development of cristae to F-ATPase dimerization (Davies et al., 2012; Paumard et al., 2002). Row- or ribbon-like formations seem to be a universal feature in mitochondrial F-ATPases. In addition to the aforementioned type I dimer rows, type II and type IV dimers, which exhibit an "intermediate" dimerization angle of ~55°, form closely spaced helical ribbons that wrap around the edges of the disk-shaped cristae of the unicellular green algae and trypanosomes (Blum et al., 2019; Mühleip et al., 2016). Molecular simulation studies have suggested that dimers spontaneously form rows in order to minimize the overall elastic strain on the IMM that arises from the local curvature imposed upon the membrane by ATPase dimerization (Anselmi et al., 2018; Davies et al., 2012). This mechanism is independent of lipid composition or any particular protein–protein interaction.

The U-shaped type III dimers found in ciliates, however, form a dimer angle close to 0°—that is, the ATPase monomers are parallel to each other. This conformation does not as obviously lend itself to the membrane deformation hypothesis as the angles of their more bent cousins. Despite this, ciliate mitochondrial membranes also show tight helical rows of dimerized ATPases, which give rise to tube-like cristae (Mühleip et al., 2016). An analogous model for the formation of these structures was proposed in which the curvature of the IMM is not simply a consequence of dimer formation, but a more specific interaction between the U-shaped dimers during row assembly. In particular, the peripheral stalks of the dimers bend the IMM, driving row formation to relieve local bending energy as in mitochondria containing V-shaped dimers (Mühleip et al., 2016). An overview of the characterized classes of ATPase dimers and their respective cristae morphologies are shown in Fig. 5.

Studies have also illustrated the importance of cristae structure on mitochondrial, and consequently on cellular and organismal, health (Bornhövd et al., 2006; Davies et al., 2012; Paumard et al., 2002). For instance, the breakdown of cristae morphology in fungal mitochondria has been associated with senescence, and comparison of cryo-electron tomography images from young and aging cultures of the fungal mold *Podospora anserina* have linked the loss of normal lamellar cristae structure to the breakdown of type I dimer rows (Daum et al., 2013). Studies in metazoan aging models demonstrated clear functional links between aging-related degradation and dimer-induced cristae ultrastructure (Brandt et al., 2017). Furthermore, in mice, changes in membrane structure were shown to be organ dependent, such that different organs exhibit different degrees of resilience against aging. For example, stacking of cristae in cardiac cells is packed more tightly than in other tissues, such as in the liver or kidney (Brandt et al., 2017).

One seemingly obvious effect of cristae packing structure is the increase of surface area in the IMM, which is important for increasing the flux of molecules across the membrane. However, elimination of regular cristae structure in yeast via mutation of subunits at the dimerization interface did not noticeably reduce inner membrane surface area, though mutants showed a significantly lower growth rate (Davies et al., 2012; Paumard et al., 2002). Other studies have implicated cristae in maintaining the mitochondrial membrane potential (Bornhövd et al., 2006; but see also Saddar et al., 2008), suggesting that cristae serve as proton-trapping "microcompartments" to aid the conveniently arranged rows of nearby ATP synthases (Daum et al., 2013; Davies et al., 2012; Davies et al., 2018; Kühlbrandt, 2019). In *Drosophila melanogaster*, dimerization of ATP synthase has been shown to be essential both for stem cell differentiation during development as well as to ward off aging-related degradation (Brandt et al., 2017; Teixeira et al., 2015).

ATP synthase has also been implicated in a more sudden and dramatic disruption of mitochondrial inner membrane structure, the mitochondrial permeability transition (PT; Bernardi, 2018; Carraro et al., 2014; Carraro et al., 2019). This transition is initiated by the Ca^{2+}-dependent opening of the mitochondrial PT pore (PTP or mPTP), a protein assembly within the IMM (Haworth and Hunter, 1979; Hunter et al., 1976). The physiological role of the mPTP is associated with calcium homeostasis, and it is likely that the pore is tasked with the governance of membrane permeability and cell fate. Disruption of these duties as a consequence of certain trauma or pathologies may result in the PT and lead to a disruption of the IMM, mitochondrial swelling, and eventual cell death (Bernardi and Bonaldo, 2008; Bernardi, 2018; Hunter et al., 1976; Massari and Azzone, 1972). Detailed studies in mammalian systems have implicated the PT in neuronal cell damage caused by excitotoxicity, neurodegenerative disease, or head injury (Fiskum, 2000; Ichas and Mazat, 1998; Schinder et al., 1996) as well as in cardiac cell damage caused by heart attack or stroke (Bopassa et al., 2005; Honda and Ping, 2006). Though the most extensive investigations of mitochondrial pore function have been in mammalian and yeast mitochondria (Jung et al., 1997; Azzolin et al., 2010; Carraro et al., 2014; He et al., 2017a, 2017b), mPTP activity has been observed in a wide range of organisms and cell types. These include sea urchin oocytes (Torrezan-Nitao et al., 2018), plants (Curtis and Wolpert, 2002), plathelminths (Song et al., 2016), nematodes (Liu et al., 2016), insects (Pan et al., 2016; Ren et al., 2017), crustaceans (Konràd et al., 2011; Konrád et al., 2012; though see, e.g., Menze et al., 2010), and birds (Vedernikov et al., 2015). The prevalence of the mPTP across lineages points to the fundamental nature of the physiological function of this complex (Azzolin et al., 2010; Uribe-Carvajal et al., 2011). The hydrolytic capacity of F-ATPase tightly connects its physiological role to the mPTP. A recent hypothesis posits that the PT originates from a conformational change in ATP synthase upon Ca^{2+} binding at the Mg^{2+} site, and has gained support through genetic and electrophysiological investigations (Alavian et al., 2014; Algieri et al., 2019; Bonora et al., 2013; Giorgio et al., 2013; Giorgio et al., 2017; Mnatsakanyan et al., 2019; Neginskaya et al., 2019; Nesci et al., 2018; Urbani et al., 2019). However, such a direct role in this transition for F-ATPases is somewhat contentious (He et al., 2017a, 2017b; Carroll et al., 2019; Karch et al., 2019).

The exact mechanisms behind the role of ATP synthase in both age- and trauma-related changes in mitochondrial structure

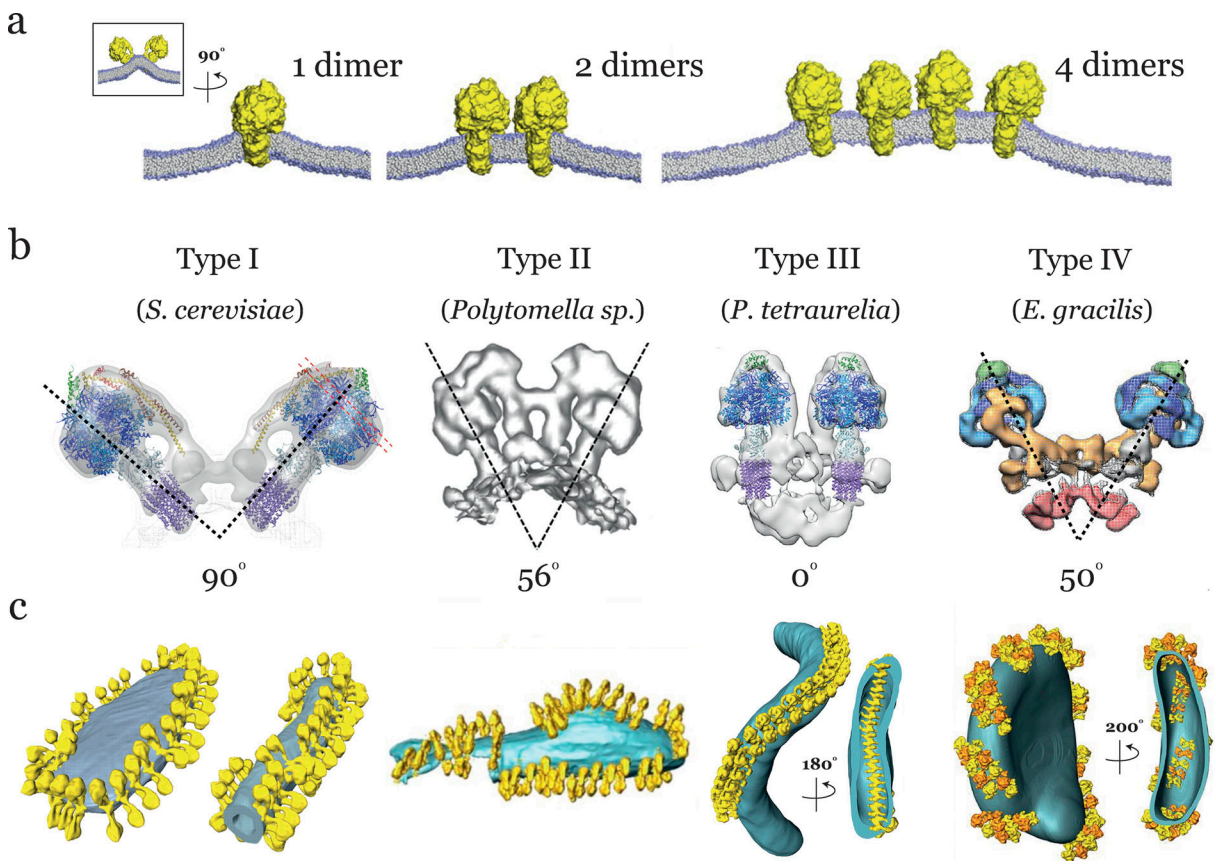

Figure 5. **Structure of mitochondrial ATP synthase dimers. (a)** Formation of dimer rows relieves strain caused by dimerization-induced local membrane curvature. Perspective slices through simulated membrane patches illustrate how curvature profile changes when one, two, or four ATP synthase dimers assemble into a row (Davies et al., 2012). **(b and c)** Subtomogram images of ATP synthase dimers (b) and surface representations of cristae structure (c) from representative species of each dimerization class: type I, *Saccharomyces cerevisiae* (Davies et al., 2012); type II, *Polytomella sp.* (reproduced with permission from Blum et al. [2019]); type III, *Paramecium tetraurelia* (Mühleip et al., 2016); type IV, *Euglena gracilis* (Mühleip et al., 2017).

and function remain largely unclear, and in some cases controversial (for an in-depth analysis of recent scholarship on the PT, see, e.g., Bernardi and Lippe 2018; Bernardi 2018; Carraro et al., 2019). More investigation in particular is needed to clarify the effects of mtF1Fo dimer formation—for instance, whether dimer dissociation is a causal agent, effect, or byproduct of senescence.

Dancing in the bilayer: Interaction of ATPases with membrane lipids

Like all membrane-embedded proteins, ATPases live in complex surroundings, the lipid building blocks of which have coevolved with their resident proteins. Thus, several open questions in bioenergetics research center around the effects and drivers of the local membrane environment (Fig. 6). In eukaryotes, distinct membrane compartments (van Meer et al., 2008) and even bilayer leaflets (Lorent et al., 2020) have their own characteristic properties based on the lipid biosynthetic and transport processes that determine their composition. The IMM is particularly unique: it is almost completely bereft of sterols and saturated sphingolipids, molecules that order and provide rigidity to the membranes and other cellular compartments. The most abundant lipid of the IMM inner leaflet is phosphatidylethanolamine (PE), while phosphatidylcholine is dominant in the outer leaflet, as it is in the rest of the cell (Colbeau et al., 1971). Even more striking is the abundance of cardiolipin (CL), a tetracyl anionic phospholipid that comprises >20% of IMMs and is exclusive to the mitochondria. Like PE, CL is enriched to the inner leaflet of the IMM (Krebs, Hauser, and Carafoli, 1979), where it comprises an even larger fraction of the lipids.

The composition of the IMM harkens back to its bacterial origins. In proteobacteria, PE is the dominant phospholipid, while CL is also synthesized, but at lower levels—CL comprises ∼5% of all lipids in *E. coli*, where it is nonessential (Nishijima et al., 1988). Thus, eukaryotic adaptations in ATPase structure and mitochondrial morphology likely coevolved alongside large-scale changes in its IMM composition, particularly the increase in CL content. Notably, the radius of curvature that characterizes cristae structures (∼15 nm) is much smaller than that of bacterial poles (∼0.5 µm), a geometric constraint that potentially underlies adaptations in both ATPase organization and lipid composition.

The biophysical properties of CL are unique among lipids and have likely led to its close association with ATPase dimers in the IMM. Containing four voluminous lipid chains, CL is regarded as a nonbilayer lipid, as it cannot form planar membranes by itself

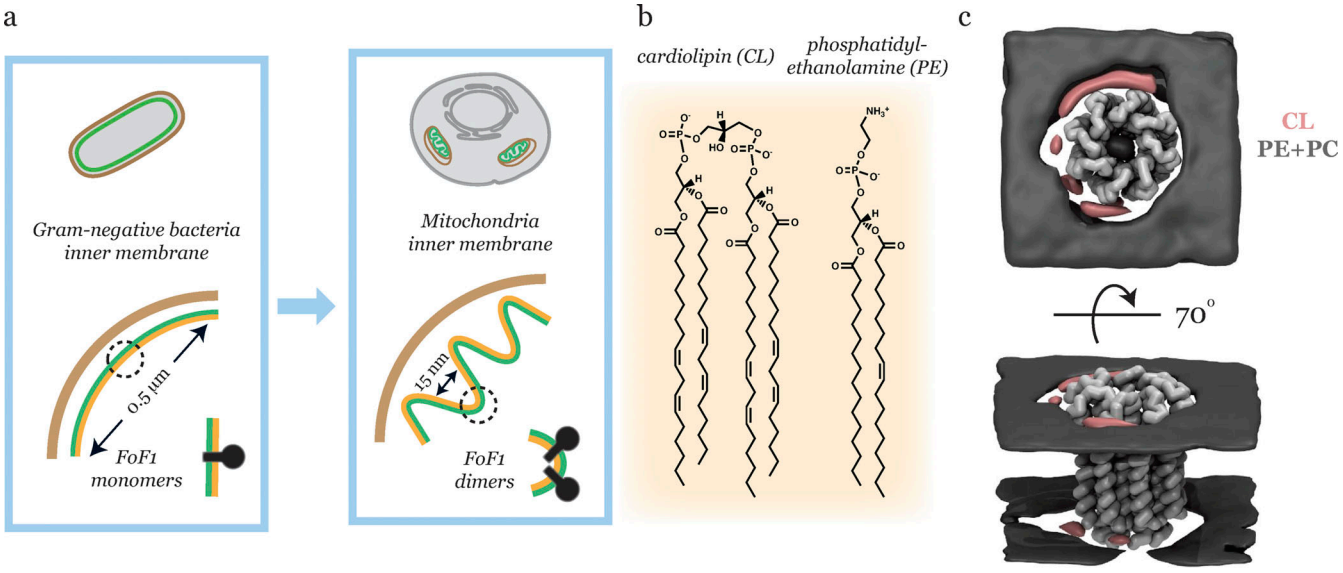

Figure 6. **Lipids associated with ATP synthase. (a)** The evolution of membrane topology from the lightly curved inner membrane of gram-negative proteobacteria to the highly curved inner membrane of eukaryotic mitochondria. For both, the inner membrane contains asymmetric distribution of lipids that provide spontaneous membrane curvature. In mitochondria, asymmetry is more dramatic and likely acts alongside the dimerization of ATP synthase to support cristae structure. **(b)** Characteristic lipids of the IMM include CL and PE. CL is shown with four linoleic acid chains, as is typical in many mammalian tissues. These lipids are also enriched on the inner leaflet of the membrane, as they are gram-negative bacteria (Bogdanov et al., 2020). **(c)** Coarse-grained MD simulations of the bovine c_8-ring in a model inner membrane suggest transient interactions with CL, whose mean density distribution is shown in pink. It has been hypothesized that these interactions promote the rotation of the ring during enzyme cycles. Figure adapted from Duncan, et al., 2016.

due to its conic shape. Pure CL instead forms hexagonal cubic and other nonlamellar phases (Ortiz et al., 1999). When incorporated into membranes, this molecular morphology imposes an intrinsic curvature, thereby facilitating the bending of highly curved structures (Alimohamadi and Rangamani, 2018; Chabanon, Stachowiak, and Rangamani, 2017). Many of the insights for this function came from studies in bacteria, where imaging with the dye nonyl acridine orange has revealed the heterogeneous distribution on CL on cell poles and division septa (Mileykovskaya and Dowhan, 2000; Kawai et al., 2004; Oliver et al., 2014). More recent studies using model membranes have demonstrated the intrinsic capability of CL to localize to thin membrane tubules (Beltrán-Heredia et al., 2019). Because the diameter of these tubules is much smaller than that of a bacterial cell, it has been proposed that domains of CL must "sense" biologically relevant curvatures (Huang et al., 2006), as in the model for curvature-sensing proteins (Ramamurthi et al., 2009). In the IMM, however, curvature is much higher at cristae edges where ATPase dimers reside, so any higher order organization is not necessary for sorting of CL to these sites. Therefore, it is generally accepted that CL is enriched at these sites, and it is possible that its enrichment allowed for the evolution of cristae structures. In one striking demonstration, the ability of mutant *E. coli* to form cristae-like internal membrane upon membrane protein overexpression was shown to be dependent on the presence of CL (Carranza et al., 2017).

Another potentially conserved function for CL is to recruit proteins to highly curved membranes, potentially through electrostatic interactions. In bacteria, deletion of CL synthase leads to the mislocalization of some polar-localized membrane proteins (Romantsov et al., 2010), suggesting a mechanism by which CL–protein interactions serve as a localization cue. In mitochondria, CL interactions have likely evolved as a mechanism for localizing mtF1Fo to cristae edges. Before models of cristae organization were developed, biochemical studies of isolated mitochondria from bovine cells found that mtF1Fo ATPase remained associated with 2.5 mol of CL, higher than all other lipids combined (Eble et al., 1990). More recent work has used genetic disruption of CL levels in several organisms to demonstrate a broad role for cristae organization (Sakamoto et al., 2012). In *Drosophila*, isolated mitochondria from flight muscle of mutants with reduced amounts of CL show slightly enlarged cristae with far fewer ATPases localizing to their edges (Acehan et al., 2011). This suggests that, at least in flies, CL has a major role in anchoring ATPases to cristae edges, but it is still unclear if CL drives cristae curvature or it acts through recruiting ATPase dimers. Better mechanical modeling of cristae membranes is needed to further understand the relative contributions both lipid composition and ATPase structure have on the IMM.

In addition to its association with curved membranes, specific lipids could act as modulators of ATPase function through biophysical effects on its mechanical cycle. Changes in CL levels modulate the respiratory cycle in biochemically isolated mitochondrial membranes (Koshkin and Greenberg, 2002), suggesting a role in dictating ETC enzyme functions. An early hypothesis is that the anionic CL can act as an intermediate proton trap that facilitates proton translocation across the bilayer (Haines and Dencher, 2002), which would also be based on transient interactions with the F-ATPase rotor ring. Unlike other

ETC complexes (Paradies et al., 2014), CL has not been observed in ATPase structures, so where would this association take place? The c-ring of metazoan ATPases feature a conserved trimethylated lysine residue (Walpole et al., 2015) that, in simulations, binds transiently to CL molecules (Duncan et al., 2016). This model (Fig. 6 c) suggests that CL interactions may have an additional stabilizing effect for the c-ring, which completes 100 rotations in the bilayer every second.

One possibility is that direct association with lipids can reduce the friction of c-ring rotation, although the mechanics of those proposals have not been fully explored. Lipids mediate the bulk hydrodynamic properties of the membranes that ATPases reside in, so aspects of lipid composition that affect membrane viscosity would affect rotational friction (Saffman and Delbrück, 1975). For example, unsaturation of phosphatidyl lipids (Budin et al., 2018) and PE head group composition (Dawaliby et al., 2016) impact membrane viscosity and could similarly influence the rotational speeds of ATPase across organisms. In metazoans, CL acyl chains are composed of highly fluidizing polyunsaturated fatty acids (Pennington et al., 2019), which are incorporated via the acyl chain remodeler Tafazzin. In humans, mutations in the gene encoding Tafazzin (*TAZ*) are the cause of Barth syndrome, an X-linked genetic disorder characterized by cardioskeletal myopathy and reduced numbers of neutrophils in the blood (Barth et al., 2004). Barth syndrome patients show a lower proportion of polyunsaturated fatty acids, such as linoleic acid, in their CL acyl chains (Schlame et al., 2002), as well as a lower level of total mitochondrial CL (Vreken et al., 2000). Mitochondria isolated from Barth syndrome patients show defects in respiratory chain supercomplex assembly (McKenzie et al., 2006), which has also been observed in yeast Tafazzin mutants (Brandner et al., 2005). However, the effects of defective CL pools are likely widespread among ETC components, including ATP synthase. Interestingly, the heart and muscle defects most commonly associated with Barth syndrome are also found in several rare genetic disorders that directly involve ATP synthase genes primarily encoded in the mitochondrial genome (Dautant et al., 2018).

Rolling forward: Conclusions and future work

Energetic considerations inform the structure, function, and evolution of cells and organisms, making the ion-translocating ATP synthase an essential and ubiquitous piece of molecular machinery. As such, small changes or defects can have catastrophic consequences, particularly in cell types whose functions necessitate the production of copious amounts of energy. These include, predictably, neurons and muscle. Indeed, several neuromuscular and neurodegenerative diseases have been linked to mitochondrial disorder and, in particular, to ATP synthase malfunction (see, e.g., Dautant et al., 2018 and Kühlbrandt, 2019 for a more comprehensive discussion). Several recent high-resolution insights into the structure of ATP synthase suggest avenues toward the development of therapies for such disorders. Further, investigations of the similarities and divergences between human mitochondrial ATPases and those of our parasites and pathogens point toward novel (and, importantly, strongly conserved) targets for antibiotic development, which may prove particularly salient in combating multidrug-resistant organisms (Chavez et al., 2020; Mitchell et al., 2020; Mühleip et al., 2016; Mühleip et al., 2017; Preiss et al., 2015).

The components of ATP synthase, especially its catalytic domains, are widely conserved from prokaryotes to plants and metazoans. The F-type ATPases in particular are responsible for bioenergetic processes in all domains of life, with members found in archaea, bacteria, and eukaryotes (Koumandou and Kossida, 2014; Mulkidjanian et al., 2007). The conserved structure and mechanism of these enzymes strongly suggest that they predate the divergence of these lineages (Rand et al., 2004), likely making ATP synthase, alongside the ribosome, among the most ancient molecular motors (Sousa et al., 2016). Though developing and testing models of early evolution is inherently challenging, there is much to be gained from understanding the origin and evolution of ATP synthase. The spread of this enzyme across the tree of life implies that the reconstruction of this lineage may also provide valuable insight into the origins of semi-permeable membranes, as these likely occurred as a coevolutionary process (Mulkidjanian et al., 2009). ATP synthase does not function in a vacuum—its interactions with its lipid environment and proteinaceous neighbors have shaped its structure and function. To this end, we hope that this review highlights the importance of considering how the complex environment of membrane proteins has impacted their function and evolutionary trajectory.

Acknowledgments

Henk L. Granzier served as editor.

J.A. Nirody is grateful for funding from the James S. McDonnell Foundation's Fellowship in Complex Systems, The Rockefeller University's Center for Studies in Physics and Biology, and All Souls College, University of Oxford; I. Budin is grateful for funding from National Science Foundation grant MCB-1715681; and P. Rangamani is grateful to the AFOSR Multidisciplinary Research Program of the University Research Initiative (MURI): Low Energy Bioinspired Information Processing.

The authors declare no competing financial interests.

Author contributions: J.A. Nirody and P. Rangamani designed the research. J.A. Nirody, I. Budin, and P. Rangamani wrote and edited the manuscript.

Submitted: 16 June 2020
Accepted: 24 August 2020

References

Acehan, D., A. Malhotra, Y. Xu, M. Ren, D.L. Stokes, and M. Schlame. 2011. Cardiolipin affects the supramolecular organization of ATP synthase in mitochondria. *Biophys. J.* 100:2184–2192. https://doi.org/10.1016/j.bpj.2011.03.031

Alavian, K.N., G. Beutner, E. Lazrove, S. Sacchetti, H.A. Park, P. Licznerski, H. Li, P. Nabili, K. Hockensmith, M. Graham, et al. 2014. An uncoupling channel within the c-subunit ring of the F1FO ATP synthase is the mitochondrial permeability transition pore. *Proc. Natl. Acad. Sci. USA.* 111:10580–10585. https://doi.org/10.1073/pnas.1401591111

Algieri, C., F. Trombetti, A. Pagliarani, V. Ventrella, C. Bernardini, M. Fabbri, M. Forni, and S. Nesci. 2019. Mitochondrial Ca^{2+}-activated F_1 F_O

-ATPase hydrolyzes ATP and promotes the permeability transition pore. *Ann. N. Y. Acad. Sci.* 1457:142–157. https://doi.org/10.1111/nyas.14218

Alimohamadi, H., and P. Rangamani. 2018. Modeling membrane curvature generation due to membrane–protein interactions. *Biomolecules*. 8:120. https://doi.org/10.3390/biom8040120

Allen, R.D. 1995. Membrane tubulation and proton pumps. *Protoplasma*. 189: 1–8. https://doi.org/10.1007/BF01280286

Angevine, C.M., K.A. Herold, and R.H. Fillingame. 2003. Aqueous access pathways in subunit a of rotary ATP synthase extend to both sides of the membrane. *Proc. Natl. Acad. Sci. USA*. 100:13179–13183. https://doi.org/10.1073/pnas.2234364100

Anselmi, C., K.M. Davies, and J.D. Faraldo-Gómez. 2018. Mitochondrial ATP synthase dimers spontaneously associate due to a long-range membrane-induced force. *J. Gen. Physiol*. 150:763–770. https://doi.org/10.1085/jgp.201812033

Azzolin, L., S. von Stockum, E. Basso, V. Petronilli, M.A. Forte, and P. Bernardi. 2010. The mitochondrial permeability transition from yeast to mammals. *FEBS Lett*. 584:2504–2509. https://doi.org/10.1016/j.febslet.2010.04.023

Banfield, J.F., and C.R. Marshall. 2000. Perspectives: earth science and evolution. Genomics and the geosciences. *Science*. 287:605–606. https://doi.org/10.1126/science.287.5453.605

Barth, P.G., F. Valianpour, V.M. Bowen, J. Lam, M. Duran, F.M. Vaz, and R.J. Wanders. 2004. X-linked cardioskeletal myopathy and neutropenia (Barth syndrome): an update. *Am. J. Med. Genet. A*. 126A:349–354. https://doi.org/10.1002/ajmg.a.20660

Bason, J.V., M.G. Montgomery, A.G. Leslie, and J.E. Walker. 2014. Pathway of binding of the intrinsically disordered mitochondrial inhibitor protein to F1-ATPase. *Proc. Natl. Acad. Sci. USA*. 111:11305–11310. https://doi.org/10.1073/pnas.1411560111

Battistuzzi, F.U., A. Feijao, and S.B. Hedges. 2004. A genomic timescale of prokaryote evolution: insights into the origin of methanogenesis, phototrophy, and the colonization of land. *BMC Evol. Biol*. 4:44. https://doi.org/10.1186/1471-2148-4-44

Beeby, M., D.A. Ribardo, C.A. Brennan, E.G. Ruby, G.J. Jensen, and D.R. Hendrixson. 2016. Diverse high-torque bacterial flagellar motors assemble wider stator rings using a conserved protein scaffold. *Proc. Natl. Acad. Sci. USA*. 113:E1917–E1926. https://doi.org/10.1073/pnas.1518952113

Beltrán-Heredia, E., F.C. Tsai, S. Salinas-Almaguer, F.J. Cao, P. Bassereau, and F. Monroy. 2019. Membrane curvature induces cardiolipin sorting. *Commun. Biol*. 2:225. https://doi.org/10.1038/s42003-019-0471-x

Bernardi, P. 2018. Why F-ATP synthase remains a strong candidate as the mitochondrial permeability transition pore. *Front. Physiol*. 9:1543. https://doi.org/10.3389/fphys.2018.01543

Bernardi, P., and P. Bonaldo. 2008. Dysfunction of mitochondria and sarcoplasmic reticulum in the pathogenesis of collagen VI muscular dystrophies. *Ann. N. Y. Acad. Sci*. 1147:303–311. https://doi.org/10.1196/annals.1427.009

Bernardi, P., and G. Lippe. 2018. Channel formation by F-ATP synthase and the permeability transition pore: an update. *Curr. Opin. Physiol*. 3:1–5. https://doi.org/10.1016/j.cophys.2017.12.006

Blum, T.B., A. Hahn, T. Meier, K.M. Davies, and W. Kühlbrandt. 2019. Dimers of mitochondrial ATP synthase induce membrane curvature and self-assemble into rows. *Proc. Natl. Acad. Sci. USA*. 116:4250–4255. https://doi.org/10.1073/pnas.1816556116

Bogdanov, M., K. Pyrshev, S. Yesylevskyy, S. Ryabichko, V. Boiko, P. Ivanchenko, R. Kiyamova, Z. Guan, C. Ramseyer, and W. Dowhan. 2020. Phospholipid distribution in the cytoplasmic membrane of Gram-negative bacteria is highly asymmetric, dynamic, and cell shape-dependent. Sci. Adv. 6:eaaz6333. https://doi.org/10.1126/sciadv.aaz6333

Bogdanović, N., D. Trifunović, H. Sielaff, L. Westphal, S. Bhushan, V. Müller, and G. Grüber. 2019. The structural features of Acetobacterium woodii F-ATP synthase reveal the importance of the unique subunit γ-loop in Na^+ translocation and ATP synthesis. *FEBS J*. 286:1894–1907. https://doi.org/10.1111/febs.14793

Bonora, M., A. Bononi, E. De Marchi, C. Giorgi, M. Lebiedzinska, S. Marchi, S. Patergnani, A. Rimessi, J.M. Suski, A. Wojtala, et al. 2013. Role of the c subunit of the FO ATP synthase in mitochondrial permeability transition. *Cell Cycle*. 12:674–683. https://doi.org/10.4161/cc.23599

Bopassa, J.C., P. Michel, O. Gateau-Roesch, M. Ovize, and R. Ferrera. 2005. Low-pressure reperfusion alters mitochondrial permeability transition. *Am. J. Physiol. Heart Circ. Physiol*. 288:H2750–H2755. https://doi.org/10.1152/ajpheart.01081.2004

Bornhövd, C., F. Vogel, W. Neupert, and A.S. Reichert. 2006. Mitochondrial membrane potential is dependent on the oligomeric state of F1F0-ATP synthase supracomplexes. *J. Biol. Chem*. 281:13990–13998. https://doi.org/10.1074/jbc.M512334200

Boucher, Y., C.J. Douady, R.T. Papke, D.A. Walsh, M.E.R. Boudreau, C.L. Nesbø, R.J. Case, and W.F. Doolittle. 2003. Lateral gene transfer and the origins of prokaryotic groups. *Annu. Rev. Genet*. 37:283–328. https://doi.org/10.1146/annurev.genet.37.050503.084247

Boyer, P.D. 1993. The binding change mechanism for ATP synthase--some probabilities and possibilities. *Biochim. Biophys. Acta*. 1140:215–250. https://doi.org/10.1016/0005-2728(93)90063-L

Boyer, P.D. 1997. The ATP synthase--a splendid molecular machine. *Annu. Rev. Biochem*. 66:717–749. https://doi.org/10.1146/annurev.biochem.66.1.717

Boyer, P.D., B. Chance, L. Ernster, P. Mitchell, E. Racker, and E.C. Slater. 1977. Oxidative phosphorylation and photophosphorylation. *Annu. Rev. Biochem*. 46:955–966. https://doi.org/10.1146/annurev.bi.46.070177.004515

Brandner, K., D.U. Mick, A.E. Frazier, R.D. Taylor, C. Meisinger, and P. Rehling. 2005. Taz1, an outer mitochondrial membrane protein, affects stability and assembly of inner membrane protein complexes: implications for Barth Syndrome. *Mol. Biol. Cell*. 16:5202–5214. https://doi.org/10.1091/mbc.e05-03-0256

Brandt, T., A. Mourier, L.S. Tain, L. Partridge, N.G. Larsson, and W. Kühlbrandt. 2017. Changes of mitochondrial ultrastructure and function during ageing in mice and *Drosophila*. *eLife*. 6:e24662. https://doi.org/10.7554/eLife.24662

Budin, I., and J.W. Szostak. 2011. Physical effects underlying the transition from primitive to modern cell membranes. *Proc. Natl. Acad. Sci. USA*. 108:5249–5254. https://doi.org/10.1073/pnas.1100498108

Budin, I., T. de Rond, Y. Chen, L.J.G. Chan, C.J. Petzold, and J.D. Keasling. 2018. Viscous control of cellular respiration by membrane lipid composition. *Science*. 362:1186–1189. https://doi.org/10.1126/science.aat7925

Cano-Estrada, A., M. Vázquez-Acevedo, A. Villavicencio-Queijeiro, F. Figueroa-Martínez, H. Miranda-Astudillo, Y. Cordeiro, J.A. Mignaco, D. Foguel, P. Cardol, M. Lapaille, et al. 2010. Subunit-subunit interactions and overall topology of the dimeric mitochondrial ATP synthase of Polytomella sp. *Biochim. Biophys. Acta*. 1797:1439–1448. https://doi.org/10.1016/j.bbabio.2010.02.024

Carranza, G., F. Angius, O. Ilioaia, A. Solgadi, B. Miroux, and I. Arechaga. 2017. Cardiolipin plays an essential role in the formation of intracellular membranes in Escherichia coli. *Biochim. Biophys. Acta Biomembr*. 1859: 1124–1132. https://doi.org/10.1016/j.bbamem.2017.03.006

Carraro, M., V. Giorgio, J. Šileikytė, G. Sartori, M. Forte, G. Lippe, M. Zoratti, I. Szabò, and P. Bernardi. 2014. Channel formation by yeast F-ATP synthase and the role of dimerization in the mitochondrial permeability transition. *J. Biol. Chem*. 289:15980–15985. https://doi.org/10.1074/jbc.C114.559633

Carraro, M., V. Checchetto, I. Szabó, and P. Bernardi. 2019. F-ATP synthase and the permeability transition pore: fewer doubts, more certainties. *FEBS Lett*. 593:1542–1553. https://doi.org/10.1002/1873-3468.13485

Carroll, J., J. He, S. Ding, I.M. Fearnley, and J.E. Walker. 2019. Persistence of the permeability transition pore in human mitochondria devoid of an assembled ATP synthase. *Proc. Natl. Acad. Sci. USA*. 116:12816–12821. https://doi.org/10.1073/pnas.1904005116

Castresana, J. 2001. Comparative genomics and bioenergetics. *Biochim. Biophys. Acta*. 1506:147–162. https://doi.org/10.1016/S0005-2728(01)00227-4

Chaban, B., I. Coleman, and M. Beeby. 2018. Evolution of higher torque in Campylobacter-type bacterial flagellar motors. *Sci. Rep*. 8:97. https://doi.org/10.1038/s41598-017-18115-1

Chabanon, M., J.C. Stachowiak, and P. Rangamani. 2017. Systems biology of cellular membranes: a convergence with biophysics. *Wiley Interdiscip. Rev. Syst. Biol. Med*. 9(5):e1386. https://doi.org/10.1002/wsbm.1386

Chavez, J.D., X. Tang, M.D. Campbell, G. Reyes, P.A. Kramer, R. Stuppard, A. Keller, H. Zhang, P.S. Rabinovitch, D.J. Marcinek, et al. 2020. Mitochondrial protein interaction landscape of SS-31. *Proc. Natl. Acad. Sci. USA*. 117:15363–15373. https://doi.org/10.1073/pnas.2002250117

Chen, I.A., and J.W. Szostak. 2004. A kinetic study of the growth of fatty acid vesicles. *Biophys. J*. 87:988–998. https://doi.org/10.1529/biophysj.104.039875

Cherepanov, D.A., A.Y. Mulkidjanian, and W. Junge. 1999. Transient accumulation of elastic energy in proton translocating ATP synthase. *FEBS Lett*. 449:1–6. https://doi.org/10.1016/S0014-5793(99)00386-5

Colbeau, A., J. Nachbaur, and P.M. Vignais. 1971. Enzymic characterization and lipid composition of rat liver subcellular membranes. *Biochim. Biophys. Acta*. 249:462–492. https://doi.org/10.1016/0005-2736(71)90123-4

Collinson, I.R., J.M. Skehel, I.M. Fearnley, M.J. Runswick, and J.E. Walker. 1996. The F1F0-ATPase complex from bovine heart mitochondria: the

molar ratio of the subunits in the stalk region linking the F1 and F0 domains. *Biochemistry*. 35:12640–12646. https://doi.org/10.1021/bi960969t

Cook, G.M., S. Keis, H.W. Morgan, C. von Ballmoos, U. Matthey, G. Kaim, and P. Dimroth. 2003. Purification and biochemical characterization of the F1Fo-ATP synthase from thermoalkaliphilic Bacillus sp. strain TA2.A1. *J. Bacteriol.* 185:4442–4449. https://doi.org/10.1128/JB.185.15.4442-4449.2003

Curtis, M.J., and T.J. Wolpert. 2002. The oat mitochondrial permeability transition and its implication in victorin binding and induced cell death. *Plant J.* 29:295–312. https://doi.org/10.1046/j.0960-7412.2001.01213.x

Daum, B., D. Nicastro, J. Austin, II, J.R. McIntosh, and W. Kühlbrandt. 2010. Arrangement of photosystem II and ATP synthase in chloroplast membranes of spinach and pea. *Plant Cell*. 22:1299–1312. https://doi.org/10.1105/tpc.109.071431

Daum, B., A. Walter, A. Horst, H.D. Osiewacz, and W. Kühlbrandt. 2013. Age-dependent dissociation of ATP synthase dimers and loss of inner-membrane cristae in mitochondria. *Proc. Natl. Acad. Sci. USA*. 110:15301–15306. https://doi.org/10.1073/pnas.1305462110

Dautant, A., T. Meier, A. Hahn, D. Tribouillard-Tanvier, J.P. di Rago, and R. Kucharczyk. 2018. ATP synthase diseases of mitochondrial genetic origin. *Front. Physiol.* 9:329. https://doi.org/10.3389/fphys.2018.00329

Davies, K.M., M. Strauss, B. Daum, J.H. Kief, H.D. Osiewacz, A. Rycovska, V. Zickermann, and W. Kühlbrandt. 2011. Macromolecular organization of ATP synthase and complex I in whole mitochondria. *Proc. Natl. Acad. Sci. USA*. 108:14121–14126. https://doi.org/10.1073/pnas.1103621108

Davies, K.M., C. Anselmi, I. Wittig, J.D. Faraldo-Gómez, and W. Kühlbrandt. 2012. Structure of the yeast F1Fo-ATP synthase dimer and its role in shaping the mitochondrial cristae. *Proc. Natl. Acad. Sci. USA*. 109:13602–13607. https://doi.org/10.1073/pnas.1204593109

Davies, K.M., T.B. Blum, and W. Kühlbrandt. 2018. Conserved in situ arrangement of complex I and III_2 in mitochondrial respiratory chain supercomplexes of mammals, yeast, and plants. *Proc. Natl. Acad. Sci. USA*. 115:3024–3029. https://doi.org/10.1073/pnas.1720702115

Davis, G.A., and D.M. Kramer. 2020. Optimization of ATP Synthase c-Rings for Oxygenic Photosynthesis. *Front Plant Sci*. 10:1778. https://doi.org/10.3389/fpls.2019.01778

Dawaliby, R., C. Trubbia, C. Delporte, C. Noyon, J.M. Ruysschaert, P. Van Antwerpen, and C. Govaerts. 2016. Phosphatidylethanolamine is a key regulator of membrane fluidity in eukaryotic cells. *J. Biol. Chem.* 291:3658–3667. https://doi.org/10.1074/jbc.M115.706523

Di Paola, M., and M. Lorusso. 2006. Interaction of free fatty acids with mitochondria: coupling, uncoupling and permeability transition. *Biochim. Biophys. Acta*. 1757:1330–1337. https://doi.org/10.1016/j.bbabio.2006.03.024

Dibrova, D.V., M.Y. Galperin, and A.Y. Mulkidjanian. 2010. Characterization of the N-ATPase, a distinct, laterally transferred Na^+-translocating form of the bacterial F-type membrane ATPase. *Bioinformatics*. 26:1473–1476. https://doi.org/10.1093/bioinformatics/btq234

Dimroth, P. 1997. Primary sodium ion translocating enzymes. *Biochim. Biophys. Acta*. 1318:11–51. https://doi.org/10.1016/S0005-2728(96)00127-2

Dimroth, P., C. von Ballmoos, and T. Meier. 2006. Catalytic and mechanical cycles in F-ATP synthases. *EMBO Rep.* 7:276–282. https://doi.org/10.1038/sj.embor.7400646

Dudkina, N.V., S. Sunderhaus, H.P. Braun, and E.J. Boekema. 2006. Characterization of dimeric ATP synthase and cristae membrane ultrastructure from Saccharomyces and Polytomella mitochondria. *FEBS Lett.* 580:3427–3432. https://doi.org/10.1016/j.febslet.2006.04.097

Dudkina, N.V., G.T. Oostergetel, D. Lewejohann, H.P. Braun, and E.J. Boekema. 2010. Row-like organization of ATP synthase in intact mitochondria determined by cryo-electron tomography. *Biochim. Biophys. Acta*. 1797:272–277. https://doi.org/10.1016/j.bbabio.2009.11.004

Duncan, A.L., A.J. Robinson, and J.E. Walker. 2016. Cardiolipin binds selectively but transiently to conserved lysine residues in the rotor of metazoan ATP synthases. *Proc. Natl. Acad. Sci. USA*. 113:8687–8692. https://doi.org/10.1073/pnas.1608396113

Eble, K.S., W.B. Coleman, R.R. Hantgan, and C.C. Cunningham. 1990. Tightly associated cardiolipin in the bovine heart mitochondrial ATP synthase as analyzed by 31P nuclear magnetic resonance spectroscopy. *J. Biol. Chem.* 265:19434–19440.

Elston, T., H. Wang, and G. Oster. 1998. Energy transduction in ATP synthase. *Nature*. 391:510–513. https://doi.org/10.1038/35185

Ethayathulla, A.S., M.S. Yousef, A. Amin, G. Leblanc, H.R. Kaback, and L. Guan. 2014. Structure-based mechanism for Na^+/melibiose symport by MelB. *Nat. Commun.* 5:3009. https://doi.org/10.1038/ncomms4009

Falk, G., and J.E. Walker. 1988. DNA sequence of a gene cluster coding for subunits of the F0 membrane sector of ATP synthase in Rhodospirillum rubrum. Support for modular evolution of the F1 and F0 sectors. *Biochem. J.* 254:109–122. https://doi.org/10.1042/bj2540109

Feniouk, B.A., M.A. Kozlova, D.A. Knorre, D.A. Cherepanov, A.Y. Mulkidjanian, and W. Junge. 2004. The proton-driven rotor of ATP synthase: ohmic conductance (10 fS), and absence of voltage gating. *Biophys. J.* 86:4094–4109. https://doi.org/10.1529/biophysj.103.036962

Feniouk, B.A., T. Suzuki, and M. Yoshida. 2006. The role of subunit epsilon in the catalysis and regulation of FOF1-ATP synthase. *Biochim. Biophys. Acta*. 1757:326–338. https://doi.org/10.1016/j.bbabio.2006.03.022

Ferguson, S.J. 2010. ATP synthase: from sequence to ring size to the P/O ratio. *Proc. Natl. Acad. Sci. USA*. 107:16755–16756. https://doi.org/10.1073/pnas.1012260107

Fischer, S., C. Etzold, P. Turina, G. Deckers-Hebestreit, K. Altendorf, and P. Gräber. 1994. ATP synthesis catalyzed by the ATP synthase of Escherichia coli reconstituted into liposomes. *Eur. J. Biochem.* 225:167–172. https://doi.org/10.1111/j.1432-1033.1994.00167.x

Fiskum, G. 2000. Mitochondrial participation in ischemic and traumatic neural cell death. *J. Neurotrauma*. 17:843–855. https://doi.org/10.1089/neu.2000.17.843

Forgac, M. 2007. Vacuolar ATPases: rotary proton pumps in physiology and pathophysiology. *Nat. Rev. Mol. Cell Biol.* 8:917–929. https://doi.org/10.1038/nrm2272

Fritz, M., A.L. Klyszejko, N. Morgner, J. Vonck, B. Brutschy, D.J. Muller, T. Meier, and V. Müller. 2008. An intermediate step in the evolution of ATPases: a hybrid F(0)-V(0) rotor in a bacterial $Na^{(+)}$ F(1)F(0) ATP synthase. *FEBS J.* 275:1999–2007. https://doi.org/10.1111/j.1742-4658.2008.06354.x

Gay, N.J., and J.E. Walker. 1981. The atp operon: nucleotide sequence of the promoter and the genes for the membrane proteins, and the δ subunit of Escherichia coli ATP-synthase. *Nucleic Acids Res.* 9:3919–3926. https://doi.org/10.1093/nar/9.16.3919

Gibbons, C., M.G. Montgomery, A.G. Leslie, and J.E. Walker. 2000. The structure of the central stalk in bovine F(1)-ATPase at 2.4 A resolution. *Nat. Struct. Biol.* 7:1055–1061. https://doi.org/10.1038/80981

Giorgio, V., S. von Stockum, M. Antoniel, A. Fabbro, F. Fogolari, M. Forte, G.D. Glick, V. Petronilli, M. Zoratti, I. Szabó, et al. 2013. Dimers of mitochondrial ATP synthase form the permeability transition pore. *Proc. Natl. Acad. Sci. USA*. 110:5887–5892. https://doi.org/10.1073/pnas.1217823110

Giorgio, V., V. Burchell, M. Schiavone, C. Bassot, G. Minervini, V. Petronilli, F. Argenton, M. Forte, S. Tosatto, G. Lippe, et al. 2017. Ca^{2+} binding to F-ATP synthase β subunit triggers the mitochondrial permeability transition. *EMBO Rep.* 18:1065–1076. https://doi.org/10.15252/embr.201643354

Giraud, M.F., P. Paumard, C. Sanchez, D. Brèthes, J. Velours, and A. Dautant. 2012. Rotor architecture in the yeast and bovine F1-c-ring complexes of F-ATP synthase. *J. Struct. Biol.* 177:490–497. https://doi.org/10.1016/j.jsb.2011.10.015

Gledhill, J.R., M.G. Montgomery, A.G. Leslie, and J.E. Walker. 2007. How the regulatory protein, IF(1), inhibits F(1)-ATPase from bovine mitochondria. *Proc. Natl. Acad. Sci. USA*. 104:15671–15676. https://doi.org/10.1073/pnas.0707326104

Gomis-Rüth, F.X., G. Moncalián, R. Pérez-Luque, A. González, E. Cabezón, F. de la Cruz, and M. Coll. 2001. The bacterial conjugation protein TrwB resembles ring helicases and F1-ATPase. *Nature*. 409:637–641. https://doi.org/10.1038/35054586

Grüber, G., M.S.S. Manimekalai, F. Mayer, and V. Müller. 2014. ATP synthases from archaea: the beauty of a molecular motor. *Biochim. Biophys. Acta*. 1837:940–952. https://doi.org/10.1016/j.bbabio.2014.03.004

Guo, H., T. Suzuki, and J.L. Rubinstein. 2019. Structure of a bacterial ATP synthase. *eLife*. 8. e43128. https://doi.org/10.7554/eLife.43128

Hahn, A., K. Parey, M. Bublitz, D.J. Mills, V. Zickermann, J. Vonck, W. Kühlbrandt, and T. Meier. 2016. Structure of a complete ATP synthase dimer reveals the molecular basis of inner mitochondrial membrane morphology. *Mol. Cell*. 63:445–456. https://doi.org/10.1016/j.molcel.2016.05.037

Hahn, A., J. Vonck, D.J. Mills, T. Meier, and W. Kühlbrandt. 2018. Structure, mechanism, and regulation of the chloroplast ATP synthase. *Science*. 360(6389). https://doi.org/10.1126/science.aat4318

Haines, T.H., and N.A. Dencher. 2002. Cardiolipin: a proton trap for oxidative phosphorylation. *FEBS Lett.* 528:35–39. https://doi.org/10.1016/S0014-5793(02)03292-1

Hargreaves, W.R., and D.W. Deamer. 1978. Liposomes from ionic, single-chain amphiphiles. *Biochemistry*. 17:3759–3768. https://doi.org/10.1021/bi00611a014

Havlíčková, V., V. Kaplanová, H. Nůsková, Z. Drahota, and J. Houštěk. 2010. Knockdown of F1 epsilon subunit decreases mitochondrial content of ATP synthase and leads to accumulation of subunit c. *Biochim. Biophys. Acta*. 1797:1124–1129. https://doi.org/10.1016/j.bbabio.2009.12.009

Haworth, R.A., and D.R. Hunter. 1979. The Ca2+-induced membrane transition in mitochondria. II. Nature of the Ca2+ trigger site. *Arch. Biochem. Biophys*. 195:460–467. https://doi.org/10.1016/0003-9861(79)90372-2

He, J., J. Carroll, S. Ding, I.M. Fearnley, and J.E. Walker. 2017a. Permeability transition in human mitochondria persists in the absence of peripheral stalk subunits of ATP synthase. *Proc. Natl. Acad. Sci. U.S.A*. 114: 9086–9091. https://doi.org/10.1073/pnas.1711201114

He, J., H.C. Ford, J. Carroll, S. Ding, I.M. Fearnley, and J.E. Walker. 2017b. Persistence of the mitochondrial permeability transition in the absence of subunit c of human ATP synthase. *Proc. Natl. Acad. Sci. U.S.A*. 114: 3409–3414. https://doi.org/10.1073/pnas.1702357114

Hedges, S.B., J. Marin, M. Suleski, M. Paymer, and S. Kumar. 2015. Tree of life reveals clock-like speciation and diversification. *Mol. Biol. Evol*. 32: 835–845. https://doi.org/10.1093/molbev/msv037

Hilario, E., and J.P. Gogarten. 1998. The prokaryote-to-eukaryote transition reflected in the evolution of the V/F/A-ATPase catalytic and proteolipid subunits. *J. Mol. Evol*. 46:703–715. https://doi.org/10.1007/PL00006351

Hohmann-Marriott, M.F., and R.E. Blankenship. 2011. Evolution of photosynthesis. *Annu. Rev. Plant Biol*. 62:515–548. https://doi.org/10.1146/annurev-arplant-042110-103811

Honda, H.M., and P. Ping. 2006. Mitochondrial permeability transition in cardiac cell injury and death. *Cardiovasc. Drugs Ther*. 20:425–432. https://doi.org/10.1007/s10557-006-0642-0

Huang, K.C., R. Mukhopadhyay, and N.S. Wingreen. 2006. A curvature-mediated mechanism for localization of lipids to bacterial poles. *PLOS Comput. Biol*. 2. e151. https://doi.org/10.1371/journal.pcbi.0020151

Hunter, D.R., R.A. Haworth, and J.H. Southard. 1976. Relationship between configuration, function, and permeability in calcium-treated mitochondria. *J. Biol. Chem*. 251:5069–5077.

Ichas, F., and J.P. Mazat. 1998. From calcium signaling to cell death: two conformations for the mitochondrial permeability transition pore. Switching from low- to high-conductance state. *Biochim. Biophys. Acta*. 1366:33–50. https://doi.org/10.1016/S0005-2728(98)00119-4

Ihara, K., T. Abe, K.I. Sugimura, and Y. Mukohata. 1992. Halobacterial A-ATP Synthase in Relation to V-ATPase. *J. Exp. Biol*. 172:475–485.

Imamura, H., M. Nakano, H. Noji, E. Muneyuki, S. Ohkuma, M. Yoshida, and K. Yokoyama. 2003. Evidence for rotation of V1-ATPase. *Proc. Natl. Acad. Sci. USA*. 100:2312–2315. https://doi.org/10.1073/pnas.0436796100

Iwabe, N., K. Kuma, M. Hasegawa, S. Osawa, and T. Miyata. 1989. Evolutionary relationship of archaebacteria, eubacteria, and eukaryotes inferred from phylogenetic trees of duplicated genes. *Proc. Natl. Acad. Sci. USA*. 86:9355–9359. https://doi.org/10.1073/pnas.86.23.9355

Jiang, W., J. Hermolin, and R.H. Fillingame. 2001. The preferred stoichiometry of c subunits in the rotary motor sector of Escherichia coli ATP synthase is 10. *Proc. Natl. Acad. Sci. USA*. 98:4966–4971. https://doi.org/10.1073/pnas.081424898

Jung, D.W., P.C. Bradshaw, and D.R. Pfeiffer. 1997. Properties of a cyclosporin-insensitive permeability transition pore in yeast mitochondria. *J. Biol. Chem*. 272:21104–21112. https://doi.org/10.1074/jbc.272.34.21104

Junge, W., H. Lill, and S. Engelbrecht. 1997. ATP synthase: an electrochemical transducer with rotatory mechanics. *Trends Biochem. Sci*. 22:420–423. https://doi.org/10.1016/S0968-0004(97)01129-8

Junge, W., H. Sielaff, and S. Engelbrecht. 2009. Torque generation and elastic power transmission in the rotary F(O)F(1)-ATPase. *Nature*. 459: 364–370. https://doi.org/10.1038/nature08145

Kagawa, Y., and E. Racker. 1966. Partial resolution of the enzymes catalyzing oxidative phosphorylation. 8. Properties of a factor conferring oligomycin sensitivity on mitochondrial adenosine triphosphatase. *J. Biol. Chem*. 241:2461–2466.

Kamp, F., D. Zakim, F. Zhang, N. Noy, and J.A. Hamilton. 1995. Fatty acid flip-flop in phospholipid bilayers is extremely fast. *Biochemistry*. 34: 11928–11937. https://doi.org/10.1021/bi00037a034

Karch, J., M.J. Bround, H. Khalil, M.A. Sargent, N. Latchman, N. Terada, P.M. Peixoto, and J.D. Molkentin. 2019. Inhibition of mitochondrial permeability transition by deletion of the ANT family and CypD. *Sci. Adv*. 5: eaaw4597. https://doi.org/10.1126/sciadv.aaw4597

Kawai, F., M. Shoda, R. Harashima, Y. Sadaie, H. Hara, and K. Matsumoto. 2004. Cardiolipin domains in *Bacillus subtilis* marburg membranes. *J. Bacteriol*. 186:1475–1483. https://doi.org/10.1128/JB.186.5.1475-1483.2004

Knoll, A.H., and J. Bauld. 1989. The evolution of ecological tolerance in prokaryotes. *Trans. R. Soc. Edinb. Earth Sci*. 80:209–223.

Kohzuma, K., C. Dal Bosco, A. Kanazawa, D.M. Kramer, and J. Meurer. 2013. A Potential Function for the γ2 Subunit (atpC2) of the Chloroplast ATP Synthase. *In* Photosynthesis Research for Food, Fuel and the Future. Springer, Berlin, Heidelberg. pp. 193–196. https://doi.org/10.1007/978-3-642-32034-7_40

Konràd, C., G. Kiss, B. Töröcsik, J.L. Lábár, A.A. Gerencser, M. Mándi, V. Adam-Vizi, and C. Chinopoulos. 2011. A distinct sequence in the adenine nucleotide translocase from Artemia franciscana embryos is associated with insensitivity to bongkrekate and atypical effects of adenine nucleotides on Ca2+ uptake and sequestration. *FEBS J*. 278:822–836. https://doi.org/10.1111/j.1742-4658.2010.08001.x

Konrád, C., G. Kiss, B. Torocsik, V. Adam-Vizi, and C. Chinopoulos. 2012. Absence of Ca2+-induced mitochondrial permeability transition but presence of bongkrekate-sensitive nucleotide exchange in C. crangon and P. serratus. *PLoS One*. 7. e39839. https://doi.org/10.1371/journal.pone.0039839

Koshkin, V., and M.L. Greenberg. 2002. Cardiolipin prevents rate-dependent uncoupling and provides osmotic stability in yeast mitochondria. *Biochem. J*. 364:317–322. https://doi.org/10.1042/bj3640317

Koumandou, V.L., and S. Kossida. 2014. Evolution of the F0F1 ATP synthase complex in light of the patchy distribution of different bioenergetic pathways across prokaryotes. *PLOS Comput. Biol*. 10. e1003821. https://doi.org/10.1371/journal.pcbi.1003821

Krah, A., D. Pogoryelov, J.D. Langer, P.J. Bond, T. Meier, and J.D. Faraldo-Gómez. 2010. Structural and energetic basis for H+ versus Na+ binding selectivity in ATP synthase Fo rotors. *Biochim. Biophys. Acta*. 1797: 763–772. https://doi.org/10.1016/j.bbabio.2010.04.014

Krebs, J.J., H. Hauser, and E. Carafoli. 1979. Asymmetric distribution of phospholipids in the inner membrane of beef heart mitochondria. *J. Biol. Chem*. 254:5308–5316.

Kühlbrandt, W. 2019. Structure and mechanisms of F-type ATP synthases. *Annu. Rev. Biochem*. 88:515–549. https://doi.org/10.1146/annurev-biochem-013118-110903

Laget, P.P., and J.B. Smith. 1979. Inhibitory properties of endogenous subunit ε in the Escherichia coli F1 ATPase. *Arch. Biochem. Biophys*. 197:83–89. https://doi.org/10.1016/0003-9861(79)90222-4

Lapierre, P., R. Shial, and J.P. Gogarten. 2006. Distribution of F- and A/V-type ATPases in Thermus scotoductus and other closely related species. *Syst. Appl. Microbiol*. 29:15–23. https://doi.org/10.1016/j.syapm.2005.06.004

Lele, P.P., B.G. Hosu, and H.C. Berg. 2013. Dynamics of mechanosensing in the bacterial flagellar motor. *Proc. Natl. Acad. Sci. USA*. 110:11839–11844. https://doi.org/10.1073/pnas.1305885110

Leone, V., and J.D. Faraldo-Gómez. 2016. Structure and mechanism of the ATP synthase membrane motor inferred from quantitative integrative modeling. *J. Gen. Physiol*. 148:441–457. https://doi.org/10.1085/jgp.201611679

Leone, V., D. Pogoryelov, T. Meier, and J.D. Faraldo-Gómez. 2015. On the principle of ion selectivity in Na^+/H^+-coupled membrane proteins: experimental and theoretical studies of an ATP synthase rotor. *Proc. Natl. Acad. Sci. USA*. 112:E1057–E1066. https://doi.org/10.1073/pnas.1421202112

Liu, Y., D. Zhi, M. Li, D. Liu, X. Wang, Z. Wu, Z. Zhang, D. Fei, Y. Li, H. Zhu, et al. 2016. Shengmai Formula suppressed over-activated Ras/MAPK pathway in C. elegans by opening mitochondrial permeability transition pore via regulating cyclophilin D. *Sci. Rep*. 6:38934. https://doi.org/10.1038/srep38934

Lorent, J.H., K.R. Levental, L. Ganesan, G. Rivera-Longsworth, E. Sezgin, M. Doktorova, E. Lyman, and I. Levental. 2020. Plasma membranes are asymmetric in lipid unsaturation, packing and protein shape. *Nat. Chem. Biol*. 16:644–652. https://doi.org/10.1038/s41589-020-0529-6

MacKenzie, K.R., J.H. Prestegard, and D.M. Engelman. 1997. A transmembrane helix dimer: structure and implications. *Science*. 276:131–133. https://doi.org/10.1126/science.276.5309.131

Martin, J.L., R. Ishmukhametov, D. Spetzler, T. Hornung, and W.D. Frasch. 2018. Elastic coupling power stroke mechanism of the F_1-ATPase molecular motor. *Proc. Natl. Acad. Sci. USA*. 115:5750–5755. https://doi.org/10.1073/pnas.1803147115

Massari, S., and G.F. Azzone. 1972. The equivalent pore radius of intact and damaged mitochondria and the mechanism of active shrinkage. *Biochim. Biophys. Acta*. 283:23–29. https://doi.org/10.1016/0005-2728(72)90094-1

McKenzie, M., M. Lazarou, D.R. Thorburn, and M.T. Ryan. 2006. Mitochondrial respiratory chain supercomplexes are destabilized in Barth Syndrome patients. *J. Mol. Biol*. 361:462–469. https://doi.org/10.1016/j.jmb.2006.06.057

Meier, T., and P. Dimroth. 2002. Intersubunit bridging by Na^+ ions as a rationale for the unusual stability of the c-rings of Na^+-translocating F1F0 ATP synthases. *EMBO Rep.* 3:1094–1098. https://doi.org/10.1093/embo-reports/kvf216

Meier, T., P. Polzer, K. Diederichs, W. Welte, and P. Dimroth. 2005a. Structure of the rotor ring of F-Type Na+-ATPase from Ilyobacter tartaricus. *Science.* 308:659–662. https://doi.org/10.1126/science.1111199

Meier, T., J. Yu, T. Raschle, F. Henzen, P. Dimroth, and D.J. Muller. 2005b. Structural evidence for a constant c11 ring stoichiometry in the sodium F-ATP synthase. *FEBS J.* 272:5474–5483. https://doi.org/10.1111/j.1742-4658.2005.04940.x

Meier, T., S.A. Ferguson, G.M. Cook, P. Dimroth, and J. Vonck. 2006. Structural investigations of the membrane-embedded rotor ring of the F-ATPase from Clostridium paradoxum. *J. Bacteriol.* 188:7759–7764. https://doi.org/10.1128/JB.00934-06

Meier, T., N. Morgner, D. Matthies, D. Pogoryelov, S. Keis, G.M. Cook, P. Dimroth, and B. Brutschy. 2007. A tridecameric c ring of the adenosine triphosphate (ATP) synthase from the thermoalkaliphilic Bacillus sp. strain TA2.A1 facilitates ATP synthesis at low electrochemical proton potential. *Mol. Microbiol.* 65:1181–1192. https://doi.org/10.1111/j.1365-2958.2007.05857.x

Meier, T., A. Krah, P.J. Bond, D. Pogoryelov, K. Diederichs, and J.D. Faraldo-Gómez. 2009. Complete ion-coordination structure in the rotor ring of Na^+-dependent F-ATP synthases. *J. Mol. Biol.* 391:498–507. https://doi.org/10.1016/j.jmb.2009.05.082

Menze, M.A., G. Fortner, S. Nag, and S.C. Hand. 2010. Mechanisms of apoptosis in Crustacea: What conditions induce versus suppress cell death? *Apoptosis.* 15:293–312. https://doi.org/10.1007/s10495-009-0443-6

Meyer zu Tittingdorf, J.M., S. Rexroth, E. Schäfer, R. Schlichting, C. Giersch, N.A. Dencher, and H. Seelert. 2004. The stoichiometry of the chloroplast ATP synthase oligomer III in Chlamydomonas reinhardtii is not affected by the metabolic state. *Biochim. Biophys. Acta.* 1659:92–99. https://doi.org/10.1016/j.bbabio.2004.08.008

Mileykovskaya, E., and W. Dowhan. 2000. Visualization of phospholipid domains in Escherichia coli by using the cardiolipin-specific fluorescent dye 10-N-nonyl acridine orange. *J. Bacteriol.* 182:1172–1175. https://doi.org/10.1128/JB.182.4.1172-1175.2000

Mitchell, W., E.A. Ng, J.D. Tamucci, K.J. Boyd, M. Sathappa, A. Coscia, M. Pan, X. Han, N.A. Eddy, E.R. May, et al. 2020. The mitochondria-targeted peptide SS-31 binds lipid bilayers and modulates surface electrostatics as a key component of its mechanism of action. *J. Biol. Chem.* 295:7452–7469. https://doi.org/10.1074/jbc.RA119.012094

Mitome, N., T. Suzuki, S. Hayashi, and M. Yoshida. 2004. Thermophilic ATP synthase has a decamer c-ring: indication of noninteger 10:3 H^+/ATP ratio and permissive elastic coupling. *Proc. Natl. Acad. Sci. USA.* 101:12159–12164. https://doi.org/10.1073/pnas.0403545101

Mnatsakanyan, N., M.C. Llaguno, Y. Yang, Y. Yan, J. Weber, F.J. Sigworth, and E.A. Jonas. 2019. A mitochondrial megachannel resides in monomeric F_1F_O ATP synthase. *Nat. Commun.* 10:5823. https://doi.org/10.1038/s41467-019-13766-2

Morales-Rios, E., M.G. Montgomery, A.G. Leslie, and J.E. Walker. 2015. Structure of ATP synthase from Paracoccus denitrificans determined by X-ray crystallography at 4.0 Å resolution. *Proc. Natl. Acad. Sci. USA.* 112:13231–13236. https://doi.org/10.1073/pnas.1517542112

Muench, S.P., J. Trinick, and M.A. Harrison. 2011. Structural divergence of the rotary ATPases. *Q. Rev. Biophys.* 44:311–356. https://doi.org/10.1017/S0033583510000338

Mühleip, A.W., F. Joos, C. Wigge, A.S. Frangakis, W. Kühlbrandt, and K.M. Davies. 2016. Helical arrays of U-shaped ATP synthase dimers form tubular cristae in ciliate mitochondria. *Proc. Natl. Acad. Sci. USA.* 113:8442–8447. https://doi.org/10.1073/pnas.1525430113

Mühleip, A.W., C.E. Dewar, A. Schnaufer, W. Kühlbrandt, and K.M. Davies. 2017. In situ structure of trypanosomal ATP synthase dimer reveals a unique arrangement of catalytic subunits. *Proc. Natl. Acad. Sci. USA.* 114:992–997. https://doi.org/10.1073/pnas.1612386114

Mukherjee, S., and A. Warshel. 2012. Realistic simulations of the coupling between the protomotive force and the mechanical rotation of the F0-ATPase. *Proc. Natl. Acad. Sci. USA.* 109:14876–14881. https://doi.org/10.1073/pnas.1212841109

Mulkidjanian, A.Y., K.S. Makarova, M.Y. Galperin, and E.V. Koonin. 2007. Inventing the dynamo machine: the evolution of the F-type and V-type ATPases. *Nat. Rev. Microbiol.* 5:892–899. https://doi.org/10.1038/nrmicro1767

Mulkidjanian, A.Y., M.Y. Galperin, and E.V. Koonin. 2009. Co-evolution of primordial membranes and membrane proteins. *Trends Biochem. Sci.* 34:206–215. https://doi.org/10.1016/j.tibs.2009.01.005

Müller, V., and G. Grüber. 2003. ATP synthases: structure, function and evolution of unique energy converters. *Cell. Mol. Life Sci.* 60:474–494. https://doi.org/10.1007/s000180300040

Müller, V., C. Ruppert, and T. Lemker. 1999. Structure and function of the A1A0-ATPases from methanogenic Archaea. *J. Bioenerg. Biomembr.* 31:15–27. https://doi.org/10.1023/A:1005451311009

Murphy, B.J., N. Klusch, J. Langer, D.J. Mills, Ö. Yildiz, and W. Kühlbrandt. 2019. Rotary substates of mitochondrial ATP synthase reveal the basis of flexible F_1-F_o coupling. *Science.* 364. https://doi.org/10.1126/science.aaw9128

Neginskaya, M.A., M.E. Solesio, E.V. Berezhnaya, G.F. Amodeo, N. Mnatsakanyan, E.A. Jonas, and E.V. Pavlov. 2019. ATP synthase C-subunit-deficient mitochondria have a small cyclosporine A-sensitive channel, but lack the permeability transition pore. *Cell Rep.* 26:11–17.e2. https://doi.org/10.1016/j.celrep.2018.12.033

Nesci, S., F. Trombetti, V. Ventrella, and A. Pagliarani. 2018. From the Ca^{2+}-activated F_1F_O-ATPase to the mitochondrial permeability transition pore: an overview. *Biochimie.* 152:85–93. https://doi.org/10.1016/j.biochi.2018.06.022

Nirody, J.A., A.L. Nord, and R.M. Berry. 2019. Load-dependent adaptation near zero load in the bacterial flagellar motor. *J. R. Soc. Interface.* 16. 20190300. https://doi.org/10.1098/rsif.2019.0300

Nishijima, S., Y. Asami, N. Uetake, S. Yamagoe, A. Ohta, and I. Shibuya. 1988. Disruption of the Escherichia coli cls gene responsible for cardiolipin synthesis. *J. Bacteriol.* 170:775–780. https://doi.org/10.1128/JB.170.2.775-780.1988

Niu, Y., S. Moghimyfiroozabad, S. Safaie, Y. Yang, E.A. Jonas, and K.N. Alavian. 2017. Phylogenetic profiling of mitochondrial proteins and integration analysis of bacterial transcription units suggest evolution of F1Fo ATP synthase from multiple modules. *J. Mol. Evol.* 85:219–233. https://doi.org/10.1007/s00239-017-9819-3

Noji, H., R. Yasuda, M. Yoshida, and K. Kinosita, Jr.. 1997. Direct observation of the rotation of F1-ATPase. *Nature.* 386:299–302. https://doi.org/10.1038/386299a0

Nord, A.L., E. Gachon, R. Perez-Carrasco, J.A. Nirody, A. Barducci, R.M. Berry, and F. Pedaci. 2017. Catch bond drives stator mechanosensitivity in the bacterial flagellar motor. *Proc. Natl. Acad. Sci. USA.* 114:12952–12957. https://doi.org/10.1073/pnas.1716002114

Oliver, P.M., J.A. Crooks, M. Leidl, E.J. Yoon, A. Saghatelian, and D.B. Weibel. 2014. Localization of anionic phospholipids in Escherichia coli cells. *J. Bacteriol.* 196:3386–3398. https://doi.org/10.1128/JB.01877-14

Ortiz, A., J.A. Killian, A.J. Verkleij, and J. Wilschut. 1999. Membrane fusion and the lamellar-to-inverted-hexagonal phase transition in cardiolipin vesicle systems induced by divalent cations. *Biophys. J.* 77:2003–2014. https://doi.org/10.1016/S0006-3495(99)77041-4

Oster, G., and H. Wang. 2000. Reverse engineering a protein: the mechanochemistry of ATP synthase. *Biochim. Biophys. Acta.* 1458:482–510. https://doi.org/10.1016/S0005-2728(00)00096-7

Oster, G., H. Wang, and M. Grabe. 2000. How Fo-ATPase generates rotary torque. *Philos. Trans. R. Soc. Lond. B Biol. Sci.* 355:523–528. https://doi.org/10.1098/rstb.2000.0593

Pan, C., Y.F. Hu, J. Song, H.S. Yi, L. Wang, Y.Y. Yang, Y.P. Wang, M. Zhang, M.H. Pan, and C. Lu. 2016. Effects of 10-hydroxycamptothecin on intrinsic mitochondrial pathway in silkworm BmN-SWU1 cells. *Pestic. Biochem. Physiol.* 127:15–20. https://doi.org/10.1016/j.pestbp.2015.09.001

Paradies, G., V. Paradies, V. De Benedictis, F.M. Ruggiero, and G. Petrosillo. 2014. Functional role of cardiolipin in mitochondrial bioenergetics. *Biochim. Biophys. Acta.* 1837:408–417. https://doi.org/10.1016/j.bbabio.2013.10.006

Paula, S., A.G. Volkov, A.N. Van Hoek, T.H. Haines, and D.W. Deamer. 1996. Permeation of protons, potassium ions, and small polar molecules through phospholipid bilayers as a function of membrane thickness. *Biophys. J.* 70:339–348. https://doi.org/10.1016/S0006-3495(96)79575-9

Paumard, P., J. Vaillier, B. Coulary, J. Schaeffer, V. Soubannier, D.M. Mueller, D. Brèthes, J.P. di Rago, and J. Velours. 2002. The ATP synthase is involved in generating mitochondrial cristae morphology. *EMBO J.* 21:221–230. https://doi.org/10.1093/emboj/21.3.221

Penefsky, H.S., M.E. Pullman, A. Datta, and E. Racker. 1960. Partial resolution of the enzymes catalyzing oxidative phosphorylation. II. Participation of a soluble adenosine tolphosphatase in oxidative phosphorylation. *J. Biol. Chem.* 235:3330–3336.

Pennington, E.R., K. Funai, D.A. Brown, and S.R. Shaikh. 2019. The role of cardiolipin concentration and acyl chain composition on mitochondrial inner membrane molecular organization and function. *Biochim. Biophys.*

Acta Mol. Cell Biol. Lipids. 1864:1039–1052. https://doi.org/10.1016/j.bbalip.2019.03.012

Pogoryelov, D., J. Yu, T. Meier, J. Vonck, P. Dimroth, and D.J. Muller. 2005. The c15 ring of the Spirulina platensis F-ATP synthase: F1/F0 symmetry mismatch is not obligatory. *EMBO Rep*. 6:1040–1044. https://doi.org/10.1038/sj.embor.7400517

Pogoryelov, D., C. Reichen, A.L. Klyszejko, R. Brunisholz, D.J. Muller, P. Dimroth, and T. Meier. 2007. The oligomeric state of c rings from cyanobacterial F-ATP synthases varies from 13 to 15. *J. Bacteriol*. 189:5895–5902. https://doi.org/10.1128/JB.00581-07

Pogoryelov, D., O. Yildiz, J.D. Faraldo-Gómez, and T. Meier. 2009. High-resolution structure of the rotor ring of a proton-dependent ATP synthase. *Nat. Struct. Mol. Biol*. 16:1068–1073. https://doi.org/10.1038/nsmb.1678

Pogoryelov, D., A.L. Klyszejko, G.O. Krasnoselska, E.M. Heller, V. Leone, J.D. Langer, J. Vonck, D.J. Müller, J.D. Faraldo-Gómez, and T. Meier. 2012. Engineering rotor ring stoichiometries in the ATP synthase. *Proc. Natl. Acad. Sci. USA*. 109:E1599–E1608. https://doi.org/10.1073/pnas.1120027109

Preiss, L., O. Yildiz, D.B. Hicks, T.A. Krulwich, and T. Meier. 2010. A new type of proton coordination in an F(1)F(o)-ATP synthase rotor ring. *PLoS Biol*. 8:e1000443. https://doi.org/10.1371/journal.pbio.1000443

Preiss, L., A.L. Klyszejko, D.B. Hicks, J. Liu, O.J. Fackelmayer, Ö. Yildiz, T.A. Krulwich, and T. Meier. 2013. The c-ring stoichiometry of ATP synthase is adapted to cell physiological requirements of alkaliphilic Bacillus pseudofirmus OF4. *Proc. Natl. Acad. Sci. USA*. 110:7874–7879. https://doi.org/10.1073/pnas.1303333110

Preiss, L., J.D. Langer, D.B. Hicks, J. Liu, O. Yildiz, T.A. Krulwich, and T. Meier. 2014. The c-ring ion binding site of the ATP synthase from Bacillus pseudofirmus OF4 is adapted to alkaliphilic lifestyle. *Mol. Microbiol*. 92:973–984. https://doi.org/10.1111/mmi.12605

Preiss, L., J.D. Langer, Ö. Yildiz, L. Eckhardt-Strelau, J.E. Guillemont, A. Koul, and T. Meier. 2015. Structure of the mycobacterial ATP synthase Fo rotor ring in complex with the anti-TB drug bedaquiline. *Sci. Adv*. 1. e1500106. https://doi.org/10.1126/sciadv.1500106

Pullman, M.E., and G.C. Monroy. 1963. A naturally occurring inhibitor of mitochondrial adenosine triphosphatase. *J. Biol. Chem*. 238:3762–3769.

Rak, M., S. Gokova, and A. Tzagoloff. 2011. Modular assembly of yeast mitochondrial ATP synthase. *EMBO J*. 30:920–930. https://doi.org/10.1038/emboj.2010.364

Ramamurthi, K.S., S. Lecuyer, H.A. Stone, and R. Losick. 2009. Geometric cue for protein localization in a bacterium. *Science*. 323:1354–1357. https://doi.org/10.1126/science.1169218

Rand, D.M., R.A. Haney, and A.J. Fry. 2004. Cytonuclear coevolution: the genomics of cooperation. *Trends Ecol. Evol. (Amst.)*. 19:645–653. https://doi.org/10.1016/j.tree.2004.10.003

Ren, X., L. Zhang, Y. Zhang, L. Mao, and H. Jiang. 2017. Mitochondria response to camptothecin and hydroxycamptothecine-induced apoptosis in Spodoptera exigua cells. *Pestic. Biochem. Physiol*. 140:97–104. https://doi.org/10.1016/j.pestbp.2017.07.003

Ressl, S., A.C. Terwisscha van Scheltinga, C. Vonrhein, V. Ott, and C. Ziegler. 2009. Molecular basis of transport and regulation in the Na(+)/betaine symporter BetP. *Nature*. 458:47–52. https://doi.org/10.1038/nature07819

Rexroth, S., J.M. Meyer Zu Tittingdorf, H.J. Schwassmann, F. Krause, H. Seelert, and N.A. Dencher. 2004. Dimeric H+-ATP synthase in the chloroplast of Chlamydomonas reinhardtii. *Biochim. Biophys. Acta*. 1658:202–211. https://doi.org/10.1016/j.bbabio.2004.05.014

Reysenbach, A.L., and E. Shock. 2002. Merging genomes with geochemistry in hydrothermal ecosystems. *Science*. 296:1077–1082. https://doi.org/10.1126/science.1072483

Richter, M.L., W.J. Patrie, and R.E. McCarty. 1984. Preparation of the epsilon subunit and epsilon subunit-deficient chloroplast coupling factor 1 in reconstitutively active forms. *J. Biol. Chem*. 259:7371–7373.

Romantsov, T., A.R. Battle, J.L. Hendel, B. Martinac, and J.M. Wood. 2010. Protein localization in Escherichia coli cells: comparison of the cytoplasmic membrane proteins ProP, LacY, ProW, AqpZ, MscS, and MscL. *J. Bacteriol*. 192:912–924. https://doi.org/10.1128/JB.00967-09

Saddar, S., M.K. Dienhart, and R.A. Stuart. 2008. The F1F0-ATP synthase complex influences the assembly state of the cytochrome bc1-cytochrome oxidase supercomplex and its association with the TIM23 machinery. *J. Biol. Chem*. 283:6677–6686. https://doi.org/10.1074/jbc.M708440200

Saffman, P.G., and M. Delbrück. 1975. Brownian motion in biological membranes. *Proc. Natl. Acad. Sci. USA*. 72:3111–3113. https://doi.org/10.1073/pnas.72.8.3111

Sakamoto, T., T. Inoue, Y. Otomo, N. Yokomori, M. Ohno, H. Arai, and Y. Nakagawa. 2012. Deficiency of cardiolipin synthase causes abnormal mitochondrial function and morphology in germ cells of Caenorhabditis elegans. *J. Biol. Chem*. 287:4590–4601. https://doi.org/10.1074/jbc.M111.314823

Schäfer, G., M. Engelhard, and V. Müller. 1999. Bioenergetics of the Archaea. *Microbiol. Mol. Biol. Rev*. 63:570–620. https://doi.org/10.1128/MMBR.63.3.570-620.1999

Schemidt, R.A., J. Qu, J.R. Williams, and W.S. Brusilow. 1998. Effects of carbon source on expression of F0 genes and on the stoichiometry of the c subunit in the F1F0 ATPase of Escherichia coli. *J. Bacteriol*. 180:3205–3208. https://doi.org/10.1128/JB.180.12.3205-3208.1998

Schinder, A.F., E.C. Olson, N.C. Spitzer, and M. Montal. 1996. Mitochondrial dysfunction is a primary event in glutamate neurotoxicity. *J. Neurosci*. 16:6125–6133. https://doi.org/10.1523/JNEUROSCI.16-19-06125.1996

Schlame, M., J.A. Towbin, P.M. Heerdt, R. Jehle, S. DiMauro, and T.J. Blanck. 2002. Deficiency of tetralinoleoyl-cardiolipin in Barth syndrome. *Ann. Neurol*. 51:634–637. https://doi.org/10.1002/ana.10176

Schlegel, K., V. Leone, J.D. Faraldo-Gómez, and V. Müller. 2012. Promiscuous archaeal ATP synthase concurrently coupled to Na^+ and H^+ translocation. *Proc. Natl. Acad. Sci. USA*. 109:947–952. https://doi.org/10.1073/pnas.1115796109

Schulz, S., M. Iglesias-Cans, A. Krah, O. Yildiz, V. Leone, D. Matthies, G.M. Cook, J.D. Faraldo-Gómez, and T. Meier. 2013. A new type of Na^+-driven ATP synthase membrane rotor with a two-carboxylate ion-coupling motif. *PLoS Biol*. 11. e1001596. https://doi.org/10.1371/journal.pbio.1001596

Schulz, S., M. Wilkes, D.J. Mills, W. Kühlbrandt, and T. Meier. 2017. Molecular architecture of the N-type ATPase rotor ring from *Burkholderia pseudomallei*. *EMBO Rep*. 18:526–535. https://doi.org/10.15252/embr.201643374

Seelert, H., and N.A. Dencher. 2011. ATP synthase superassemblies in animals and plants: two or more are better. *Biochim. Biophys. Acta*. 1807:1185–1197. https://doi.org/10.1016/j.bbabio.2011.05.023

Smith, J.B., P.C. Sternweis, and L.A. Heppel. 1975. Partial purification of active delta and epsilon subunits of the membrane ATPase from escherichia coli. *J. Supramol. Struct*. 3:248–255. https://doi.org/10.1002/jss.400030307

Sobti, M., C. Smits, A.S. Wong, R. Ishmukhametov, D. Stock, S. Sandin, and A.G. Stewart. 2016. Cryo-EM structures of the autoinhibited *E. coli* ATP synthase in three rotational states. *eLife*. 5. https://doi.org/10.7554/eLife.21598

Song, Y., L. Huang, and J. Yu. 2016. Effects of blueberry anthocyanins on retinal oxidative stress and inflammation in diabetes through Nrf2/HO-1 signaling. *J. Neuroimmunol*. 301:1–6. https://doi.org/10.1016/j.jneuroim.2016.11.001

Song, J., N. Pfanner, and T. Becker. 2018. Assembling the mitochondrial ATP synthase. *Proc. Natl. Acad. Sci. USA*. 115:2850–2852. https://doi.org/10.1073/pnas.1801697115

Sousa, F.L., S. Nelson-Sathi, and W.F. Martin. 2016. One step beyond a ribosome: The ancient anaerobic core. *Biochim. Biophys. Acta*. 1857:1027–1038. https://doi.org/10.1016/j.bbabio.2016.04.284

Steed, P.R., and R.H. Fillingame. 2008. Subunit a facilitates aqueous access to a membrane-embedded region of subunit c in Escherichia coli F1F0 ATP synthase. *J. Biol. Chem*. 283:12365–12372. https://doi.org/10.1074/jbc.M800901200

Steed, P.R., and R.H. Fillingame. 2009. Aqueous accessibility to the transmembrane regions of subunit c of the Escherichia coli F1F0 ATP synthase. *J. Biol. Chem*. 284:23243–23250. https://doi.org/10.1074/jbc.M109.002501

Stock, D., C. Gibbons, I. Arechaga, A.G. Leslie, and J.E. Walker. 2000. The rotary mechanism of ATP synthase. *Curr. Opin. Struct. Biol*. 10:672–679. https://doi.org/10.1016/S0959-440X(00)00147-0

Strauss, M., G. Hofhaus, R.R. Schröder, and W. Kühlbrandt. 2008. Dimer ribbons of ATP synthase shape the inner mitochondrial membrane. *EMBO J*. 27:1154–1160. https://doi.org/10.1038/emboj.2008.35

Sun, S.X., H. Wang, and G. Oster. 2004. Asymmetry in the F1-ATPase and its implications for the rotational cycle. *Biophys. J*. 86:1373–1384. https://doi.org/10.1016/S0006-3495(04)74208-3

Symersky, J., V. Pagadala, D. Osowski, A. Krah, T. Meier, J.D. Faraldo-Gómez, and D.M. Mueller. 2012. Structure of the c(10) ring of the yeast mitochondrial ATP synthase in the open conformation. *Nat. Struct. Mol. Biol*. 19:485–491: S1. https://doi.org/10.1038/nsmb.2284

Teixeira, F.K., C.G. Sanchez, T.R. Hurd, J.R. Seifert, B. Czech, J.B. Preall, G.J. Hannon, and R. Lehmann. 2015. ATP synthase promotes germ cell

differentiation independent of oxidative phosphorylation. *Nat. Cell Biol.* 17:689–696. https://doi.org/10.1038/ncb3165

Torrezan-Nitao, E., R.C.B.Q. Figueiredo, and L.F. Marques-Santos. 2018. Mitochondrial permeability transition pore in sea urchin female gametes. *Mech. Dev.* 154:208–218. https://doi.org/10.1016/j.mod.2018.07.008

Tzagoloff, A. 1969. Assembly of the mitochondrial membrane system. II. Synthesis of the mitochondrial adenosine triphosphatase. F1. *J. Biol. Chem.* 244:5027–5033.

Urbani, A., V. Giorgio, A. Carrer, C. Franchin, G. Arrigoni, C. Jiko, K. Abe, S. Maeda, K. Shinzawa-Itoh, J.F.M. Bogers, et al. 2019. Purified F-ATP synthase forms a Ca^{2+}-dependent high-conductance channel matching the mitochondrial permeability transition pore. *Nat. Commun.* 10:4341. https://doi.org/10.1038/s41467-019-12331-1

Uribe-Carvajal, S., L.A. Luévano-Martínez, S. Guerrero-Castillo, A. Cabrera-Orefice, N.A. Corona-de-la-Peña, and M. Gutiérrez-Aguilar. 2011. Mitochondrial Unselective Channels throughout the eukaryotic domain. *Mitochondrion.* 11:382–390. https://doi.org/10.1016/j.mito.2011.02.004

van Lis, R., D. González-Halphen, and A. Atteia. 2005. Divergence of the mitochondrial electron transport chains from the green alga Chlamydomonas reinhardtii and its colorless close relative Polytomella sp. *Biochim. Biophys. Acta.* 1708:23–34. https://doi.org/10.1016/j.bbabio.2004.12.010

van Lis, R., G. Mendoza-Hernández, G. Groth, and A. Atteia. 2007. New insights into the unique structure of the F0F1-ATP synthase from the chlamydomonad algae Polytomella sp. and Chlamydomonas reinhardtii. *Plant Physiol.* 144:1190–1199. https://doi.org/10.1104/pp.106.094060

van Meer, G., D.R. Voelker, and G.W. Feigenson. 2008. Membrane lipids: where they are and how they behave. *Nat. Rev. Mol. Cell Biol.* 9:112–124. https://doi.org/10.1038/nrm2330

Vázquez-Acevedo, M., P. Cardol, A. Cano-Estrada, M. Lapaille, C. Remacle, and D. González-Halphen. 2006. The mitochondrial ATP synthase of chlorophycean algae contains eight subunits of unknown origin involved in the formation of an atypical stator-stalk and in the dimerization of the complex. *J. Bioenerg. Biomembr.* 38:271–282. https://doi.org/10.1007/s10863-006-9046-x

Vedernikov, A.A., M.V. Dubinin, V.A. Zabiakin, and V.N. Samartsev. 2015. Ca^{2+}-dependent nonspecific permeability of the inner membrane of liver mitochondria in the guinea fowl (Numida meleagris). *J. Bioenerg. Biomembr.* 47:235–242. https://doi.org/10.1007/s10863-015-9606-z

Vinothkumar, K.R., M.G. Montgomery, S. Liu, and J.E. Walker. 2016. Structure of the mitochondrial ATP synthase from *Pichia angusta* determined by electron cryo-microscopy. *Proc. Natl. Acad. Sci. USA.* 113:12709–12714. https://doi.org/10.1073/pnas.1615902113

Vollmar, M., D. Schlieper, M. Winn, C. Büchner, and G. Groth. 2009. Structure of the c14 rotor ring of the proton translocating chloroplast ATP synthase. *J. Biol. Chem.* 284:18228–18235. https://doi.org/10.1074/jbc.M109.006916

von Ballmoos, C., A. Wiedenmann, and P. Dimroth. 2009. Essentials for ATP synthesis by F1F0 ATP synthases. *Annu. Rev. Biochem.* 78:649–672. https://doi.org/10.1146/annurev.biochem.78.081307.104803

Vreken, P., F. Valianpour, L.G. Nijtmans, L.A. Grivell, B. Plecko, R.J. Wanders, and P.G. Barth. 2000. Defective remodeling of cardiolipin and phosphatidylglycerol in Barth syndrome. *Biochem. Biophys. Res. Commun.* 279:378–382. https://doi.org/10.1006/bbrc.2000.3952

Wadhwa, N., R. Phillips, and H.C. Berg. 2019. Torque-dependent remodeling of the bacterial flagellar motor. *Proc. Natl. Acad. Sci. USA.* 116:11764–11769.

Walker, J.E. 1998. ATP synthesis by rotary catalysis (Nobel Lecture). *Angew. Chem. Int. Ed. Engl.* 37:2308–2319. https://doi.org/10.1002/(SICI)1521-3773(19980918)37:17<2308::AID-ANIE2308>3.0.CO;2-W

Walpole, T.B., D.N. Palmer, H. Jiang, S. Ding, I.M. Fearnley, and J.E. Walker. 2015. Conservation of complete trimethylation of lysine-43 in the rotor ring of c-subunits of metazoan adenosine triphosphate (ATP) synthases. *Mol. Cell. Proteomics.* 14:828–840. https://doi.org/10.1074/mcp.M114.047456

Wang, H., and G. Oster. 1998. Energy transduction in the F1 motor of ATP synthase. *Nature.* 396:279–282. https://doi.org/10.1038/24409

Watt, I.N., M.G. Montgomery, M.J. Runswick, A.G. Leslie, and J.E. Walker. 2010. Bioenergetic cost of making an adenosine triphosphate molecule in animal mitochondria. *Proc. Natl. Acad. Sci. USA.* 107:16823–16827. https://doi.org/10.1073/pnas.1011099107

Weber, J., and A.E. Senior. 2003. ATP synthesis driven by proton transport in F1F0-ATP synthase. *FEBS Lett.* 545:61–70. https://doi.org/10.1016/S0014-5793(03)00394-6

Wilkens, S., and R.A. Capaldi. 1998. ATP synthase's second stalk comes into focus. *Nature.* 393:29. https://doi.org/10.1038/29908

Xing, J., J.C. Liao, and G. Oster. 2005. Making ATP. *Proc. Natl. Acad. Sci. USA.* 102:16539–16546. https://doi.org/10.1073/pnas.0507207102

Yamashita, A., S.K. Singh, T. Kawate, Y. Jin, and E. Gouaux. 2005. Crystal structure of a bacterial homologue of Na^+/Cl--dependent neurotransmitter transporters. *Nature.* 437:215–223. https://doi.org/10.1038/nature03978

Yanagisawa, S., and W.D. Frasch. 2017. Protonation-dependent stepped rotation of the F-type ATP synthase c-ring observed by single-molecule measurements. *J. Biol. Chem.* 292:17093–17100. https://doi.org/10.1074/jbc.M117.799940

Yasuda, R., H. Noji, M. Yoshida, K. Kinosita, Jr., and H. Itoh. 2001. Resolution of distinct rotational substeps by submillisecond kinetic analysis of F1-ATPase. *Nature.* 410:898–904. https://doi.org/10.1038/35073513

Zhou, A., A. Rohou, D.G. Schep, J.V. Bason, M.G. Montgomery, J.E. Walker, N. Grigorieff, and J.L. Rubinstein. 2015. Structure and conformational states of the bovine mitochondrial ATP synthase by cryo-EM. *eLife.* 4. e10180. https://doi.org/10.7554/eLife.10180

Zhu, T.F., and J.W. Szostak. 2009. Coupled growth and division of model protocell membranes. *J. Am. Chem. Soc.* 131:5705–5713. https://doi.org/10.1021/ja900919c

Zimniak, L., P. Dittrich, J.P. Gogarten, H. Kibak, and L. Taiz. 1988. The cDNA sequence of the 69-kDa subunit of the carrot vacuolar H^+-ATPase. Homology to the beta-chain of F0F1-ATPases. *J. Biol. Chem.* 263:9102–9112.